

<https://doi.org/10.3799/dqkx.2021.088>



# 金属稳定同位素示踪地球增氧事件

王振飞, 黄康俊\*, 路雅雯, 罗 瑾, 鞠鹏程, 蒙泽坤

大陆动力学国家重点实验室, 陕西省早期生命与环境重点实验室, 西北大学地质学系, 陕西西安 710069

**摘 要:** 早期贫氧地球如何演化至现今富氧地球是理解地球宜居性形成与演化的关键, 但重建地质历史时期地球大气与海洋氧含量仍是地球科学领域的重大挑战. 金属稳定同位素的高精度测试分析为示踪地球大气与海洋氧化历史提供了新的研究手段. 以 Mo、U、Tl、Cr 四种氧化还原敏感金属稳定同位素体系为例, 详细介绍了氧化还原敏感金属稳定同位素地球化学行为及分馏机理. 在此基础上, 系统回顾了金属稳定同位素在研究产氧光合作用的起源、大氧化事件(Great Oxidation Event, GOE)、中元古代大气和海洋氧化还原状态、新元古代氧化事件(NOE)等重大科学问题中的研究进展. 金属稳定同位素在重建地球表层圈层氧化过程具有广阔的应用前景, 对认识地球宜居性的演化历史以及探索其未来发展趋势具有深远意义.

**关键词:** 氧循环; 地球宜居性; 氧化还原敏感金属元素; 产氧光合作用; 大氧化事件; 中元古代; 新元古代氧化事件; 地球化学.

中图分类号: P581

文章编号: 1000-2383(2021)12-4427-25

收稿日期: 2021-04-21

## Tracing Earth's Oxygenation Events Using Metal Stable Isotopes

Wang Zhenfei, Huang Kangjun\*, Lu Yawen, Luo Jin, Ju Pengcheng, Meng Zekun

State Key Laboratory of Continental Dynamics, Shaanxi Key Laboratory of Early Life and Environments, Department of Geology, Northwest University, Xi'an 710069, China

**Abstract:** How early anoxic earth evolved to modern oxidic Earth is the key to understand the formation and evolution of Earth's habitability. However, reconstructions of atmospheric and oceanic oxygen levels over Earth's history are still significant challenges. The high precision analysis of redox sensitive metal stable isotopes provides a powerful means to trace Earth's oxygenation history. In this review, it takes Mo, U, Tl, Cr isotopes as example to introduce the geochemical behaviors and fractionation mechanism of redox sensitive metal stable isotope systems. On this basis, it systematically reviews the advances of metal stable isotopes in important research issues including the onset of oxygenic photosynthesis, Great Oxidation Event (GOE), the redox state of atmosphere and ocean in the Mesoproterozoic, Neoproterozoic Oxidation Event (NOE). Metal stable isotopes have great application prospects in reconstructing the oxidation processes of Earth's surface. Furthermore, metal stable isotopes have profound significance in understanding the evolution of Earth's habitability and exploring its development in the future.

**Key words:** oxygen cycle; Earth's habitability; redox sensitive metal element; oxygenic photosynthesis; Great Oxidation Event (GOE); Mesoproterozoic; Neoproterozoic Oxidation Event (NOE); geochemistry.

## 0 引言

随着现今自然环境问题日益突出, 地球宜居性的形成与演化已经成为地球科学研究领域的热点

问题. 在现代富氧地球上, 除厌氧生物外几乎所有的生命都需要氧气来进行新陈代谢和维持生命活动. 因此, 氧循环是影响地球宜居性的重要因素(黄

**基金项目:** 国家自然科学基金项目(Nos.41973008, 41890845, 41621003); 中国科学院“西部之光”交叉团队项目(No.E0290101).

**作者简介:** 王振飞(1997-), 男, 硕士研究生, 研究方向为前寒武纪古环境演化. ORCID:0000-0003-2979-8397. E-mail: wangzhenfei184@163.com

\* **通讯作者:** 黄康俊, E-mail: hkj@nwu.edu.cn

**引用格式:** 王振飞, 黄康俊, 路雅雯, 等, 2021. 金属稳定同位素示踪地球增氧事件. 地球科学, 46(12):4427-4451.

建平等, 2021).

氧(O)是宇宙中丰度仅次于H和He的元素(Anders and Grevesse, 1989),在地壳中丰度最高.现代大气氧含量高达21%,但在地球形成最初的二十多亿年,大气氧含量不足 $10^{-5}$  PAL(present atmosphere level)(Holland, 2006)(图1).化石记录以及生物标志化合物证据均指示产氧光合作用出现时间不晚于3.0 Ga(Allwood *et al.*, 2006; Knoll *et al.*, 2016)(图1).之后在2.4~2.3 Ga,大气氧含量显著增高,达到1%~10% PAL,被称为大氧化事件(Great Oxidation Event, GOE)(Catling *et al.*, 2001; Holland, 2007; Lyons *et al.*, 2014).直至新元古代晚期,地球经历了第二次氧化事件(Neoproterozoic Oxidation Event, NOE),大气与海洋氧含量升高至显生宙水平(Sperling *et al.*, 2015),促进了后生动物的出现与辐射(朱茂炎, 2010; Erwin *et al.*, 2011; Li *et al.*, 2018; 赵相宽等, 2018; 朱茂炎等, 2019)(图1).

地球氧含量增加从根本上改变了地球表层环境,深刻影响了生物圈的演化进程(殷鸿福等, 2018).因此,恢复地质历史时期大气与海洋氧气水平是探索生命与环境协同演化过程的关键科学问题.

对地球表层圈层氧化历史的认识很大程度上依赖于地球化学指标的发展.早期的研究,铁组分(Canfield *et al.*, 2008; Poulton *et al.*, 2010)、微量元素富集程度(Scott *et al.*, 2008; Sahoo *et al.*, 2012)、硫同位素(Fike and Grotzinger, 2008; Fike *et al.*, 2015)、氮同位素(Stüeken *et al.*, 2015, 2016)等地球化学指标对重建地球氧化还原状态发挥了重要的作用.然而,这些传统地球化学指标大多提供的是局部环境的氧化还原信息,并且在定量重建全球大气与海洋氧化还原状态方面存在不足(周锡强等, 2017).新世纪以来,随着多接收等离子体质谱(MC-ICP-MS)测试分析技术的革新和发展,实现了氧化还原敏感金属稳定同位素高精度测试分析,为研究

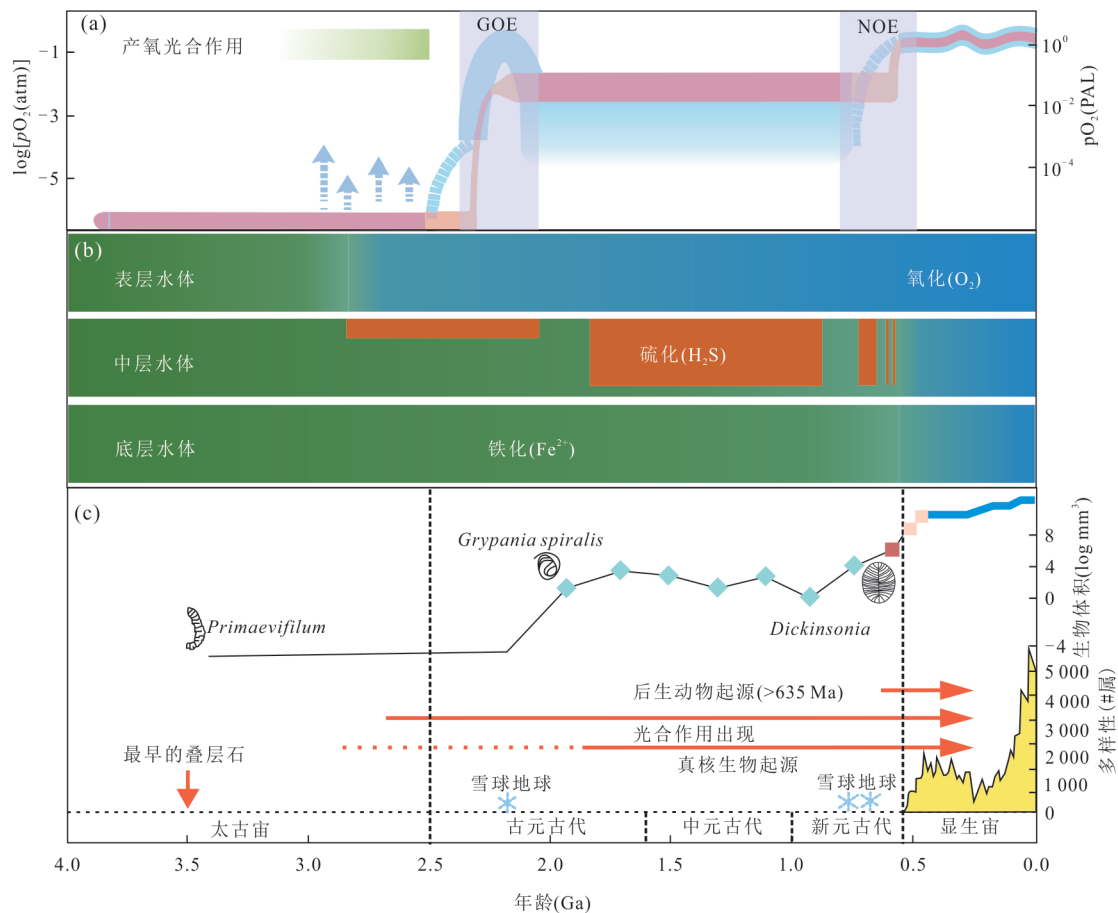


图1 地质历史时期大气氧气浓度变化(a)与海洋氧化还原条件变化(b)及生物演化重大事件(c)

Fig.1 The evolution of atmospheric oxygen levels (a), marine redox states (b), as well as the major biological innovative events (c) during the geological history

修改自 Shields-Zhou and Och(2011); Lyons *et al.*(2014); Poulton(2017)

地球大气与海洋氧化历史提供了新的研究手段(朱祥坤等, 2013). 一方面, 氧化还原敏感金属稳定同位素体系在表生地质过程中一般会产生显著的同位素分馏(Kendall, 2021; Anbar and Rouxel, 2007), 并且这些分馏过程往往与大气海洋氧化还原状态联系密切. 例如 Mo、U 和 Cr 等元素随着氧化还原状态波动会发生价态变化, 进而引起同位素显著分馏; 氧化环境下形成的 Mn 氧化物通过吸附作用也会导致 Mo 和 Tl 同位素发生明显分馏. 另一方面, 在现代海洋中这些金属元素的滞留时间远大于全球海水的混合时间( $\sim 1\sim 2$  ka)(Sarmiento and Gruber, 2006). 因此, 相较于传统地球化学指标, 氧化还原敏感金属稳定同位素在恢复地质历史时期全球海洋氧化还原程度更具优势.

本文以 Mo、U、Tl 和 Cr 同位素为例, 系统介绍了氧化还原敏感金属稳定同位素的地球化学行为及其分馏机理. 在此基础上, 重点阐述氧化还原敏感金属稳定同位素在以下方面的研究进展: 产氧光合作用起源, GOE 期间大气与海洋氧化程度, 中元古代大气氧含量与真核生物演化之间的潜在联系, NOE 对后生动物起源与辐射的可能影响. 最后, 分析了氧化还原敏感金属稳定同位素体系在研究地球增氧事件中存在的问题, 并展望了未来的发展前景.

## 1 氧化还原敏感金属稳定同位素分馏机理

地球化学指标示踪地球氧化过程主要是利用不同元素对氧化还原反应的敏感程度存在差异(图 2). 根据元素在不同氧化还原环境下的赋存状态与溶解度的关系, 氧化还原敏感元素大致可分为 3 类(Algeo and Li, 2020; Kendall, 2021): 第一类元素的氧化态易溶于氧化水体中, 但难溶于缺氧水体中(例如, Mo、U、Cr 等); 第二类则表现出相反的地球化学行为, 其氧化态不溶于氧化的水体中, 但还原态易溶于缺氧的水体中(例如, Fe、Mn 等); 第三类元素的氧化态和还原态都溶于水, 例如 Tl 元素, 在氧化的环境中氧化态 Tl 会被 Mn 氧化物强烈吸附, 使水体中溶解 Tl 以还原态为主. 在前寒武纪缺氧海洋中,  $\text{Fe}^{2+}$  和  $\text{Mn}^{2+}$  浓度较高, 滞留时间可达到百万年(Ma)(Johnson and Beard, 2006). 相较于 Fe、Mn 元素, Mo、U、Tl、Cr 元素在缺氧海洋中滞留时间更短, 因此, 理论上对于早期地球氧化还原状态变化响应更加敏感.

### 1.1 Mo 同位素地球化学性质

Mo 有 7 个稳定同位素, 即  $^{92}\text{Mo}$ 、 $^{94}\text{Mo}$ 、 $^{95}\text{Mo}$ 、 $^{96}\text{Mo}$ 、 $^{97}\text{Mo}$ 、 $^{98}\text{Mo}$  和  $^{100}\text{Mo}$ , 其平均自然丰度分别为 14.84%、9.25%、15.92%、16.68%、9.55%、24.13% 和 9.63%. 一般使用  $\delta^{98}\text{Mo}$  来表示 Mo 同位素组

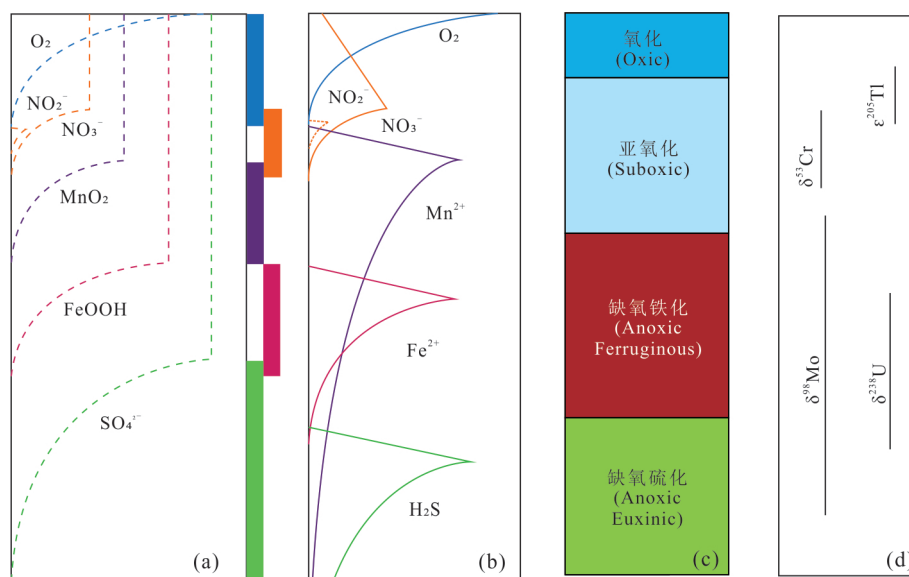


图 2 氧化还原梯度带与氧化还原敏感金属稳定同位素关系概念

Fig.2 Conceptual figure of the relationship between redox gradient zone and redox sensitive metal stable isotopes

a. 早成岩阶段普通电子受体深度分布图; b. 早成岩阶段厌氧代谢产物深度分布图; c. 氧化还原条件深度变化; d. 在不同的氧化还原相带下氧化还原敏感金属稳定同位素响应区间; 修改自 Canfield and Thamdrup(2009); Kendall(2021); Owens(2019)

成(表 1).

Mo 是现代海洋中丰度最高的过渡金属元素 (~107 nmol/kg), 主要以钼酸盐( $\text{MoO}_4^{2-}$ )的形式存在, 且不易与其他离子形成配位(Collier, 1985). Mo 在现代海洋中的滞留时间约为 440 ka, 较全球海水混合时间更长(Miller *et al.*, 2011). 因此, 全球海水具有均一的  $\delta^{98}\text{Mo}$  值 ( $2.34\text{‰} \pm 0.10\text{‰}$ ) (Barling *et al.*, 2001; Siebert *et al.*, 2003; 朱建明等, 2008; Nakagawa *et al.*, 2012)(图 3). 海洋中的 Mo 超过 90% 来源于河流输入, 也有大约 5% 来自海底热液(Neely *et al.*, 2018). 通过河流输入的  $\delta^{98}\text{Mo}$  变化较大 ( $-0.1\text{‰} \sim 2.3\text{‰}$ ) (Archer and Vance, 2008; Pearce *et al.*, 2010; Neubert *et al.*, 2011), 平均值为  $0.7\text{‰}$ , 大于平均上地壳值 ( $0.15\text{‰}$ ) (Archer and Vance, 2008; 程猛等, 2015; Willbold and Elliott, 2017). 海洋中 Mo 的汇从大到小排列依次为亚氧化环境沉积物 (50%)、氧化环境沉积物 (40%)、硫化环境沉积物 (10%) (Scott *et al.*, 2008; Reinhard *et al.*, 2013).

研究表明海水中 Mo 同位素的分馏主要受控于局部水体的氧化还原状态: 在氧化水体中, Mo 同位素受 Fe-Mn 氧化物吸附作用的影响发生较大的分馏. 其中, Mo 同位素受 Mn 氧化物吸附作用产生的分馏比 Fe 氧化物更大, 分馏值最大可达到  $-3\text{‰}$  (Barling *et al.*, 2001; Siebert *et al.*, 2003; Wasylenki *et al.*, 2008). 在现代氧化大洋背景下, 深海中形成的铁锰结壳吸附了海水中大量轻的 Mo, 导致海水 Mo 同位素相对上地壳更重. 在亚氧化环境(孔隙水硫化)中, 由于将 Mo 输送到沉积物中的氧化物类型以及孔隙水  $\text{H}_2\text{S}$  浓度不同, Mo 同位素的分馏是可变的 ( $\Delta^{98}\text{Mo} = -3.0\text{‰} \sim -0.3\text{‰}$ ), 平均值为  $-0.8\text{‰}$  (Siebert *et al.*, 2006; Poulson Brucker *et al.*, 2009; Goldberg *et al.*, 2012; Poulson Brucker *et al.*, 2012).

在硫化环境中, Mo 同位素的分馏系数变化很大 ( $-3.0\text{‰} \sim -0.3\text{‰}$ ), 这可能与水体硫化程度以及 Fe-Mn 氧化物搬运机(Fe-Mn shuttle)作用的影响有关(Neubert *et al.*, 2008; Nögler *et al.*, 2011; Noordmann *et al.*, 2015; Andersen *et al.*, 2018; Scholz *et al.*, 2018). 在硫化程度不同的水体中, Mo 的赋存形式会随着水体硫化程度的增强而逐步转化:  $\text{MoO}_4^{2-} \rightarrow \text{MoO}_3\text{S}_2^{2-} \rightarrow \text{MoO}_2\text{S}_2^{2-} \rightarrow \text{MoOS}_3^{2-} \rightarrow \text{MoS}_4^{2-} \rightarrow \text{MoS}_2$  (Erickson and Helz, 2000), 并在转化过程中发生不同程度的分馏:  $\Delta^{98}\text{Mo}_{0,1} = \Delta^{98}\text{Mo}_{1,2} = 1.20\text{‰}$ ,  $\Delta^{98}\text{Mo}_{2,3} = \Delta^{98}\text{Mo}_{3,4} = 1.5\text{‰}$  (其中 1, 2, 3, 4 代表  $\text{MoO}_{4-x}\text{S}_x^{2-}$  中的  $x$ ) (Tosell, 2005). 然而, 在强硫化的水体环境中(水体  $\text{H}_2\text{S}$  浓度大于  $11 \mu\text{M}$ , 例如现代黑海), 底层水中溶解的 Mo 完全转变成  $\text{MoS}_2/\text{MoS}_4^{2-}$  进入沉积物, 此过程 Mo 同位素分馏程度较小(Barling *et al.*, 2001; Arnold *et al.*, 2004; Neubert *et al.*, 2008). 因此, 强硫化水体环境下形成的沉积物可以记录开阔大洋的 Mo 同位素组成, 是重建全球海水氧化还原状态的理想载体.

## 1.2 U 同位素地球化学性质

U 有 3 个稳定同位素, 即  $^{234}\text{U}$ 、 $^{235}\text{U}$ 、 $^{238}\text{U}$ , 其平均自然丰度分别为  $0.5\%$ 、 $7.2\%$ 、 $99.3\%$  (Andersen *et al.*, 2017), 一般使用  $\delta^{238}\text{U}$  表示 U 同位素组成(表 1). U 在现代海洋中以溶解态的  $\text{U}^{6+}$  为主, 滞留时间约为 450 ka, 长于全球海水混合时间(Dunk *et al.*, 2002). 因此, 现代海洋具有相对均一的  $\delta^{238}\text{U}$  组成 ( $-0.39\text{‰} \pm 0.02\text{‰}$ ) (Andersen *et al.*, 2014; Tissot and Dauphas, 2015)(图 3). 海洋中 U 主要来源于河流输入, 其  $\delta^{238}\text{U}$  平均值为  $-0.3\text{‰}$ , 与上地壳和地幔的平均组成接近(Andersen *et al.*, 2015; Tissot and Dauphas, 2015; Andersen *et al.*, 2016; Andersen

表 1 Mo、U、Tl、Cr 同位素组成表示方式

Table 1 The expressions of Mo, U, Tl, Cr isotopes

同位素体系	表示方式	标样	参考文献
Mo	$\delta^{98}\text{Mo}(\text{‰}) = \left( \frac{(^{98}\text{Mo}/^{95}\text{Mo})_{\text{sample}}}{(^{98}\text{Mo}/^{95}\text{Mo})_{\text{SRM3134}}} - 1 \right) \times 1000 + 0.25$	NIST SRM-3134	Kendall <i>et al.</i> (2017)
U	$\delta^{238}\text{U}(\text{‰}) = \left( \frac{(^{238}\text{U}/^{235}\text{U})_{\text{sample}}}{(^{238}\text{U}/^{235}\text{U})_{\text{CRM145}}} - 1 \right) \times 1000$	NIST CRM-145	Andersen <i>et al.</i> (2017)
Tl	$\epsilon^{205}\text{Tl} = \left( \frac{(^{205}\text{Tl}/^{203}\text{Tl})_{\text{sample}}}{(^{205}\text{Tl}/^{203}\text{Tl})_{\text{SRM997}}} - 1 \right) \times 10000$	NIST SRM-997	Nielsen <i>et al.</i> (2017)
Cr	$\delta^{53}\text{Cr}(\text{‰}) = \left( \frac{(^{53}\text{Cr}/^{52}\text{Cr})_{\text{sample}}}{(^{53}\text{Cr}/^{52}\text{Cr})_{\text{SRM979}}} - 1 \right) \times 1000$	NIST SRM-979	Qin and Wang(2017)

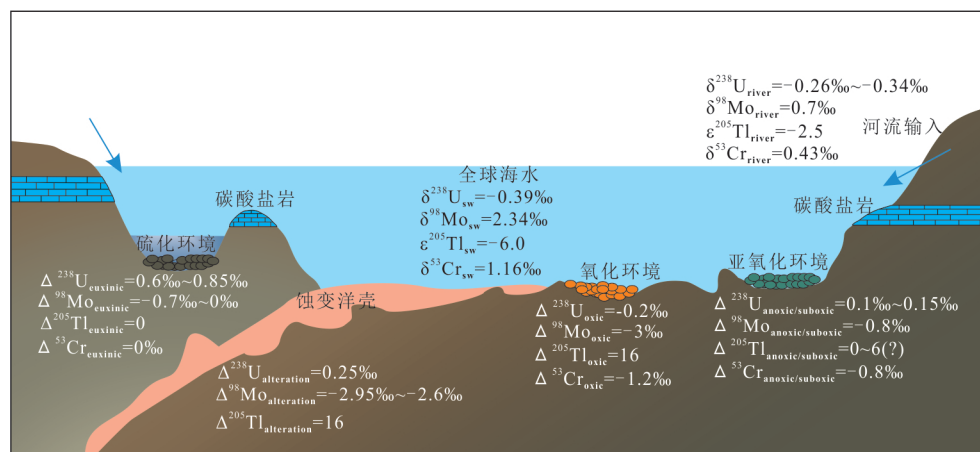


图3 现代海洋系统中Mo、U、Tl和Cr同位素循环

Fig.3 Global cycles of Mo, U, Tl and Cr isotopes in the modern oceans.

$\Delta Y_X = \delta Y_X - \delta Y_{\text{sw}}$ , 其中Y代表氧化还原元素,X代表不同元素不同的汇;数据来源:Mo同位素(Barling *et al.*, 2001; Siebert *et al.*, 2003; Archer and Vance, 2008; Wasylenko *et al.*, 2008; Nägler *et al.*, 2011; Poulson Brucker *et al.*, 2012; Scholz *et al.*, 2018; Ahmad *et al.*, 2021); U同位素(Dunk *et al.*, 2002; Andersen *et al.*, 2014, 2015, 2016, 2017; Tissot *et al.*, 2018; Zhang *et al.*, 2020); Tl同位素(Nielsen *et al.*, 2005, 2006a, 2006b, 2017; Peacock and Moon, 2012; Owens *et al.*, 2017); Cr同位素(Jeandel and Minster, 1987; Reinhard *et al.*, 2013; Gueguen *et al.*, 2016; Paulukat *et al.*, 2016; Goring-Harford *et al.*, 2018; Wei *et al.*, 2018b)

*et al.*, 2017). 海洋中U的汇由大到小排列依次为缺氧水体沉积物(46%)、碳酸盐岩(23%)、低温洋壳蚀变(23%)以及Fe-Mn氧化物的吸附(8%)(Tissot and Dauphas, 2015; Lau *et al.*, 2019).

海洋中U同位素分馏主要受水体氧化还原状态控制.在缺氧水体中,U<sup>6+</sup>被还原成U<sup>4+</sup>时,<sup>238</sup>U优先进入缺氧沉积物(Schauble, 2007; Stylo *et al.*, 2015; Brown *et al.*, 2018).其中,在硫化水体环境中,沉积物与海水分馏值最大,现代观测指示该过程U同位素分馏值( $\Delta$ )为0.5‰~0.7‰(Andersen *et al.*, 2014).但在非硫化缺氧环境下U同位素分馏系数还未得到很好的限定(Cole *et al.*, 2020).在氧化水体中,溶解态的U以铀酰酸根(UO<sub>2</sub><sup>2+</sup>)和铀酰碳酸根(UO<sub>2</sub>(CO<sub>3</sub>)<sub>3</sub><sup>4-</sup>)为主,很容易进入碳酸盐岩晶格之中.因此,碳酸盐岩被认为是记录海水 $\delta^{238}\text{U}$ 最可靠的载体.但是在孔隙水硫化环境中,早成岩过程仍会引起碳酸盐岩 $\delta^{238}\text{U}$ 产生0.24‰~0.27‰的分馏(Chen *et al.*, 2018; Tissot *et al.*, 2018).并且后期重结晶过程也会导致碳酸盐岩 $\delta^{238}\text{U}$ 发生微小偏差(Hood *et al.*, 2016).尽管如此,在考虑成岩作用影响后,碳酸盐岩 $\delta^{238}\text{U}$ 仍被认为是重建海水氧化还原状态较为可靠的指标.在缺少碳酸盐岩沉积记录的情况下,富有机质页岩 $\delta^{238}\text{U}$ 也常被用来反映全球海水氧化还原状态(Lau *et al.*, 2019).但是由于底水中溶解的U<sup>6+</sup>很难完全被还原成U<sup>4+</sup>进入缺氧沉

积物,黑色页岩 $\delta^{238}\text{U}$ 不仅包含了全球海水 $\delta^{238}\text{U}$ 信息,也记录了局部水体的氧化还原状态.因此,利用黑色页岩 $\delta^{238}\text{U}$ 恢复古海洋氧化还原状态需要准确扣除局部分馏信号(Lau *et al.*, 2019).

### 1.3 Tl同位素地球化学性质

Tl有2个稳定同位素,即<sup>203</sup>Tl、<sup>205</sup>Tl,其平均自然丰度分别为30%、70%(Nielsen *et al.*, 2017).一般使用 $\epsilon^{205}\text{Tl}$ 表示Tl同位素组成(表1).Tl在现代海洋中的滞留时间约为20 ka,同样长于全球海水混合时间(Nielsen *et al.*, 2017).但相较于Mo和U, Tl在海洋中滞留时间更短,且具有更高的氧化还原电势(Eh)(图2).因此,理论上Tl同位素比Mo和U同位素对海洋氧化还原条件变化更加敏感(Nielsen *et al.*, 2011; Ostrander *et al.*, 2017; Them *et al.*, 2018; Bowman *et al.*, 2019).Tl在地球表层环境中以+3和+1两种价态存在,并且Tl<sup>3+</sup>和Tl<sup>+</sup>都表现出高度的流体活动性.在现代氧化的海洋中,Tl主要以Tl<sup>+</sup>存在,而氧化态Tl<sup>3+</sup>会被Mn氧化物尤其是水钠锰矿强烈吸附(Peacock and Moon, 2012; Nielsen *et al.*, 2013),现代海水 $\epsilon^{205}\text{Tl}$ 为-6(Nielsen *et al.*, 2017).现代海洋中的Tl主要来自河流输入、火山去气、热液流体、沉积物孔隙水以及矿物气溶胶等.这些主要来源的 $\epsilon^{205}\text{Tl}$ 值与地幔值(-2)接近(Nielsen *et al.*, 2005; Nielsen *et al.*, 2006a).因此,海洋中Tl的来源改变不会引起海水 $\epsilon^{205}\text{Tl}$ 值的变化

(图 3). 然而, 海洋 Tl 输入通量的变化会改变海水中 Tl 的滞留时间 (Nielsen *et al.*, 2006b; Owens *et al.*, 2017).

海洋中溶解 Tl 主要有两种输出方式, 即低温洋壳蚀变以及 Mn 氧化物的吸附 (Nielsen *et al.*, 2017), 两者占现代海洋 Tl 输出通量的 95% 以上. 低温洋壳蚀变过程移除的 Tl 约占 63%, 这个过程不会产生显著的同位素分馏, 其  $\epsilon^{205}\text{Tl}$  平均值为  $-7.5$ , 与海水接近 (图 3). Mn 氧化物吸附移除的 Tl 约占 32%, 这个过程会引起 Tl 同位素显著分馏, 分馏值 ( $\Delta$ ) 最高可达 16 (Nielsen *et al.*, 2017; Owens *et al.*, 2017) (图 3). 因此, Mn 氧化物埋藏通量的变化会对海洋  $\epsilon^{205}\text{Tl}$  产生重要的影响. 海洋 Mn 氧化物的埋藏通量与海洋氧化程度密切相关, 因此, 海水 Tl 同位素组成可以反映地质历史时期海洋氧化还原状态变化. 现有研究认为, 与开阔大洋连通较好沉积盆地的硫化水体沉积物可以记录海水  $\epsilon^{205}\text{Tl}$  组成 (Nielsen *et al.*, 2011). 然而, 局限盆地的硫化水体沉积物不能记录开阔大洋海水 Tl 同位素值, 这可能是由于局限盆地与开阔大洋水体交换程度低, 海水  $\epsilon^{205}\text{Tl}$  主要受控于局部河流的输入 (Nielsen *et al.*, 2011; Owens *et al.*, 2017). 因此, 在恢复古海洋  $\epsilon^{205}\text{Tl}$  变化时必须考虑沉积盆地局限性的影响.

#### 1.4 Cr 同位素地球化学性质

Cr 有 4 个稳定同位素, 即  $^{50}\text{Cr}$ 、 $^{52}\text{Cr}$ 、 $^{53}\text{Cr}$ 、 $^{54}\text{Cr}$ , 其平均自然丰度分别为 4.35%、83.79%、9.50%、2.36% (王相力和卫炜, 2020). 一般使用  $\delta^{53}\text{Cr}$  来表示 Cr 同位素组成 (表 1). Cr 在自然界中主要有  $\text{Cr}^{3+}$  和  $\text{Cr}^{6+}$  两个价态, 在有氧风化作用下, 上地壳中不溶的  $\text{Cr}^{3+}$  氧化形成可溶的铬酸根 ( $\text{HCrO}_4^-$ ,  $\text{CrO}_4^{2-}$ ) 进入流体相, 通过河流和地下水输入海洋 (Kotaš and Stasicka, 2000), 这一过程通常需要 Mn 氧化物参与 (Eary and Rai, 1987; Fendorf *et al.*, 1992), 同时伴随着显著的 Cr 同位素分馏, 即重 Cr 同位素优先富集于  $\text{Cr}^{6+}$  中 (图 3). 在铬酸根迁移过程中, 部分溶解态  $\text{Cr}^{6+}$  被还原态的 Fe 或者溶解态的  $\text{H}_2\text{S}$  还原成  $\text{Cr}^{3+}$ , 这个过程中轻的 Cr 同位素优先进入沉积物中, 导致流体相更加富集重 Cr 同位素 (Zink *et al.*, 2010). 此外, 水体 pH 变化以及有机质络合作用会引起 Cr 同位素发生微小分馏, 但是由水体氧化还原状态变化引起的 Cr 同位素分馏程度更大 (Yusof *et al.*, 2007).

Cr 在现代海洋中主要以  $\text{HCrO}_4^-$  和  $\text{CrO}_4^{2-}$  形式存在, 滞留时间为 6.3 ka (Wei *et al.*, 2018b), 长于海

水混合时间. 由于海洋局部氧化还原环境的差异, 不同区域海水  $\delta^{53}\text{Cr}$  值高度不均一 (王相力和卫炜, 2020). 但是现代整体大洋的铬元素及同位素循环处于平衡状态, 海水  $\delta^{53}\text{Cr}$  平均为  $1.16\text{‰} \pm 0.27\text{‰}$  (Goring-Harford *et al.*, 2018) (图 3). 海水中超过 98% Cr 源自河流输入, 其  $\delta^{53}\text{Cr}$  平均值为  $0.47\text{‰}$  (Toma *et al.*, 2019), 大于整体硅酸盐地球  $\delta^{53}\text{Cr}$  值 ( $-0.124\text{‰} \pm 0.1\text{‰}$ ) (Schoenberg *et al.*, 2008). 海水中 Cr 的汇由高到低分别为亚氧化沉积物 (89.1%)、氧化沉积物 (6.7%)、缺氧沉积物 (4.2%) (Reinhard *et al.*, 2014). 由于缺乏亚氧化沉积物 Cr 同位素数据, 亚氧化环境中 Cr 还原过程同位素分馏系数还未很好限定. 在氧化环境中, Mn 氧化物优先吸附水体中轻的 Cr 同位素, 造成海水与铁锰结壳之间发生显著的 Cr 同位素分馏, 分馏值 ( $\Delta$ ) 可达  $-1.2\text{‰}$  (Wei *et al.*, 2018b). 在缺氧环境中,  $\text{Cr}^{6+}$  会被还原态物质迅速还原为  $\text{Cr}^{3+}$  形成沉淀, 该过程不会导致缺氧沉积物与海水  $\delta^{53}\text{Cr}$  之间发生明显分馏 (Reinhard *et al.*, 2014; Gueguen *et al.*, 2016). 因此, 黑色页岩  $\delta^{53}\text{Cr}$  可以记录海水 Cr 同位素组成 (Cole *et al.*, 2016). 在缺氧铁化的水体中,  $\text{Cr}^{6+}$  会被水体  $\text{Fe}^{2+}$  快速且完全还原成  $\text{Cr}^{3+}$ , 并与 Fe 氧化物或氢氧化物共同沉淀. 因此, 富铁沉积物 (包括铁建造和铁岩) 是记录海水 Cr 同位素组成的重要载体 (Frei *et al.*, 2009; Planavsky *et al.*, 2014b). 此外, 海水中溶解的  $\text{HCrO}_4^-$  和  $\text{CrO}_4^{2-}$  可以在不改变化合价态情况下进入碳酸盐岩晶格中, 且不发生明显的同位素分馏. 碳酸盐岩  $\delta^{53}\text{Cr}$  可以反映海水 Cr 同位素组成 (Gilleaudeau *et al.*, 2016). 因此, 铁建造、页岩以及碳酸盐岩等海相沉积物的 Cr 同位素组成常被用来反演地质历史时期大气和海洋氧化还原状态.

## 2 在示踪地球增氧事件中的应用

本章节以 Mo、U、Tl、Cr 四种氧化还原敏感金属稳定同位素体系为例, 围绕产氧光合作用起源、大氧化事件、中元古代大气与海洋增氧事件、新元古代氧化事件等重大地质事件, 探讨金属稳定同位素在示踪地球增氧事件中的研究进展及其发展潜力.

### 2.1 产氧光合作用起源时间

产氧光合作用是地球表层圈层自由氧的最主要来源, 因此, 限定产氧光合作用起源时间对研究地球氧化历程具有重要科学意义. 然而, 由于难以

区分早期的氧化作用是由生物作用控制还是非生物作用控制(Lyons *et al.*, 2014), 目前对于产氧光合作用出现的时间并未取得一致认识, 时间跨度从 38 亿年到 23.5 亿年(Rosing and Frei, 2004; Kirschvink and Kopp, 2008; Fischer *et al.*, 2016). 其中有无自由氧的参与是两种氧化作用最重要的区别. 近年来, 金属稳定同位素在解决这一科学问题上取得了重要进展, 主要通过示踪有氧风化作用出现来限定产氧光合作用起源时间. 此外, 金属稳定同位素在恢复太古宙海洋氧化程度方面也作出了重大贡献.

**2.1.1 有氧风化作用出现时间** 有氧风化作用是指在大气自由氧参与下, 赋存在大陆地壳中还原态物质转化为氧化态的过程. 由于大气中自由氧主要来自于产氧光合作用, 因此, 有氧风化出现的最早时间基本上可以代表产氧光合作用起源时间的下限(Kendall, 2021). 在有氧风化作用的过程中, 赋存在上地壳中的  $\text{Mo}^{4+}$ 、 $\text{U}^{4+}$ 、 $\text{Cr}^{3+}$  等还原态物质被氧化为可溶的  $\text{MoO}_4^{2-}$ 、 $\text{UO}_2^{2+}$ 、 $\text{HCrO}_4^-$ , 通过河流输入到海洋中. 这些过程会产生明显的同位素分馏(Romaniello *et al.*, 2013; Stylo *et al.*, 2015; Hinojosa *et al.*, 2016; Rolison *et al.*, 2017). 因此, 通过 Mo、U、Cr 同位素可以示踪有氧风化作用开始时间.

目前, 来自 Mo、U、Cr 同位素的证据将产氧光合作用起源时间限制在 3.0~2.9 Ga 和 2.7~2.5 Ga 两个时期. 对南非 Pongola 超群 2.95 Ga 富 Mn 铁建造研究发现,  $\delta^{98}\text{Mo}$  与 Fe/Mn 之间存在正相关关系(Planavsky *et al.*, 2014a; Ossa Ossa *et al.*, 2018b), 表明当时浅海环境中存在溶解态的  $\text{MoO}_4^{2-}$ , 在氧化环境下形成的 Mn 氧化物通过吸附作用引起海水 Mo 同位素强烈分馏. 由于 Mn 具有较高的 Eh 值, 在水体中除  $\text{H}_2\text{O}_2$  外,  $\text{O}_2$  是唯一可以将  $\text{Mn}^{2+}$  氧化为  $\text{Mn}^{4+}$  的氧化剂. 据此, 研究人员预测产氧光合作用在 2.95 Ga 就已经出现, 并在海洋表层形成氧气绿洲(Planavsky *et al.*, 2014a). 由于海洋中  $\text{Mn}^{2+}$  非生物氧化动力学过程非常缓慢, 他们进一步推断在 GOE 之前浅海环境中氧化代谢微生物已经出现, 对浅海富 Mn 铁建造沉积具有重要的控制作用(Ossa Ossa *et al.*, 2018b). 此外, 对地质历史时期沉积物 U 同位素组成统计发现, 黑色页岩  $\delta^{238}\text{U}$  在 3.0 Ga 开始增大, 逐渐偏离上地壳  $\delta^{238}\text{U}$  范围(图 4). 这表明在 3.0 Ga 时大气氧含量升高, 大量  $\text{U}^{6+}$  输入到海洋, 使黑色页岩中含 U 自生矿物逐渐增加. 此外, 由于  $\text{U}^{6+}$  不完全还原作用,  $^{238}\text{U}$  优先进入缺氧沉积物中, 导致

黑色页岩  $\delta^{238}\text{U}$  增加(Wang *et al.*, 2018). 同时 BIF 和古土壤的 U 同位素组成在 3.0 Ga 呈现极负的值, 这可能是由于 Fe-Mn 氧化物对于对流体相中  $^{235}\text{U}$  优先吸附引起的(Wang *et al.*, 2018). 基于此, 研究人员推测在 3.0 Ga 大陆开始经历大规模有氧风化作用, 产氧光合作用可能在该时期已经出现(Wang *et al.*, 2018). 此外, 南非 Pongola 超群(2.96 Ga) 古土壤  $\delta^{53}\text{Cr}$  显著低于整体硅酸盐地球值, 而同时期沉积的条带状铁建造  $\delta^{53}\text{Cr}$  高于整体硅酸盐地球值(Crowe *et al.*, 2013)(图 4). 这表明在有氧风化过程中, 重的  $^{53}\text{Cr}$  优先进入流体相并迁移至海洋, 造成风化残余的古土壤相对亏损  $\delta^{53}\text{Cr}$ . 因此, Crowe *et al.* (2013) 认为产氧光合作用至少在 GOE 发生之前 6 亿年就已经出现, 并且当时大气氧含量至少达到 0.03% PAL. 然而, Lalonde and Konhauser(2015) 却提出 2.96 Ga 古土壤较低的  $\delta^{53}\text{Cr}$  值可能是由早期陆地上微生物席中蓝细菌产生的氧气氧化导致的, 并不能指示当时大气中出现了氧气. 最近, Albut *et al.* (2018) 指出 Crowe *et al.* (2013) 采集的样品来自露头剖面, 古土壤低的  $\delta^{53}\text{Cr}$  值有可能受到现代有氧风化作用的影响.

然而, 另外一些研究表明在 2.7 Ga 之前大气氧含量较低, 有氧风化作用较弱, 广泛的产氧光合作用可能还没有出现(Siebert *et al.*, 2005; Wille *et al.*, 2007, 2013; Brüske *et al.*, 2020). 研究人员对西澳以及南非地区太古宇沉积地层(3.4~2.7 Ga) 进行氧化还原敏感金属稳定同位素研究, 结果表明部分地层  $\delta^{98}\text{Mo}$ 、 $\delta^{238}\text{U}$ 、 $\delta^{53}\text{Cr}$  值均与上地壳值接近, 且沉积物中 Mo、U、Cr 含量与上地壳一致(Wille *et al.*, 2013; Brüske *et al.*, 2020). 但是对西澳地区 Mt. McRae 组页岩(2.5 Ga) Mo 同位素测试结果表明, 该层位  $\delta^{98}\text{Mo}$  大于上地壳平均值(0.7‰), 沉积物 Mo 含量大于上地壳值, 且部分黑色页岩  $\delta^{98}\text{Mo}$  达到 1.86‰. 据此, Duan *et al.* (2010) 认为有氧风化作用至少在 2.5 Ga 时已经出现. 此外, 该层位 U 同位素组成同样显著高于上地壳  $\delta^{238}\text{U}$  值( $-0.31\text{‰} \pm 0.14\text{‰}$ ), 但沉积物 U 含量与上地壳一致. 因此, 研究人员推测 2.5 Ga 大气氧含量虽然可以氧化硫化物矿物, 但还不足以氧化晶质铀矿( $\text{UO}_2$ )(Kendall *et al.*, 2013). 相反, 由于海洋中氧气绿洲的存在, 在浅海沉积物中碎屑晶质铀矿会被海水中的氧气氧化, 以  $\text{U}^{6+}$  释放到海水中(Kendall *et al.*, 2013).

总的来说, 通过金属同位素示踪有氧风化作用

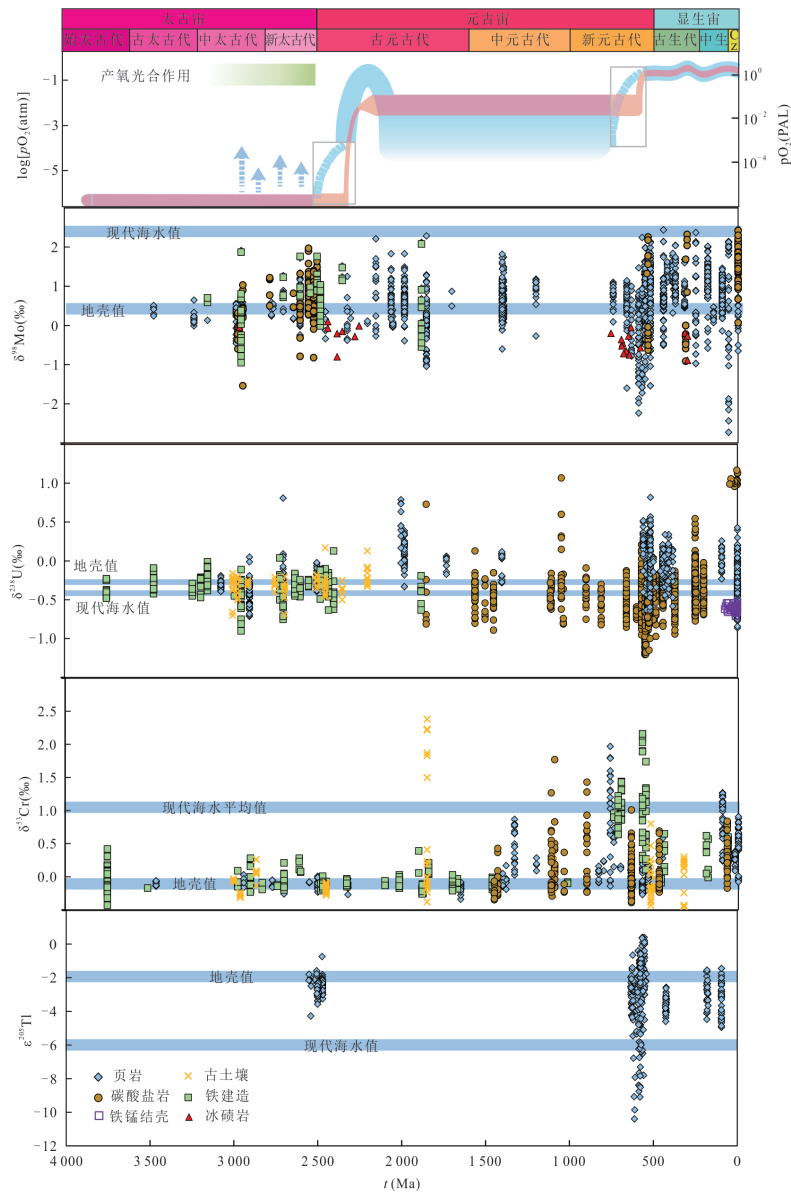


图4 地质历史时期沉积物Mo、U、Tl、Cr同位素组成演化图解

Fig.4 Mo, U, Tl and Cr isotopic compositions of sediments through geological time

CZ为新生代;地壳U同位素值与现代海水U同位素平均值接近;数据来源:Mo同位素(Barling *et al.*, 2001; Siebert *et al.*, 2003, 2005, 2006; Arnold *et al.*, 2004; Lehmann *et al.*, 2007; Wille *et al.*, 2007; Gordon *et al.*, 2009; Voegelin *et al.*, 2009; Duan *et al.*, 2010; Pearce *et al.*, 2010; Scheiderich *et al.*, 2010; Voegelin *et al.*, 2010; Dahl *et al.*, 2011; Kendall *et al.*, 2011; Neubert *et al.*, 2011; Zhou *et al.*, 2011; Dickson *et al.*, 2012; Herrmann *et al.*, 2012; Xu *et al.*, 2012; Zhou *et al.*, 2012; Asael *et al.*, 2013, 2018; Wille *et al.*, 2013; Planavsky *et al.*, 2014a; Chen *et al.*, 2015; Eroglu *et al.*, 2015; Kendall *et al.*, 2015, 2020; Kurzweil *et al.*, 2015a, 2015b, 2016; Wen *et al.*, 2015; Cheng *et al.*, 2016, 2017, 2018; Romaniello *et al.*, 2016; Diamond *et al.*, 2018; Ossa Ossa *et al.*, 2018a; Planavsky *et al.*, 2018; Scholz *et al.*, 2018; Dong *et al.*, 2019; Ostrander *et al.*, 2019b; Thoby *et al.*, 2019; Zhang *et al.*, 2019c; Gilleaudeau *et al.*, 2020; Greaney *et al.*, 2020; Mänd *et al.*, 2020; Stockey *et al.*, 2020; Ye *et al.*, 2020; Tan *et al.*, 2021); U同位素(Montoya-Pino *et al.*, 2010; Brenneka *et al.*, 2011; Asael *et al.*, 2013; Kendall *et al.*, 2013, 2015; Dahl *et al.*, 2014; Holmden *et al.*, 2015; Noordmann *et al.*, 2015; Wang *et al.*, 2016, 2018; Elrick *et al.*, 2017; Jost *et al.*, 2017; Lau *et al.*, 2017; Lu *et al.*, 2017; Song *et al.*, 2017; Yang *et al.*, 2017; Bartlett *et al.*, 2018; Phan *et al.*, 2018; Wei *et al.*, 2018a; White *et al.*, 2018; Zhang *et al.*, 2018a, 2018b, 2018c, 2018d, 2019a; Dahl *et al.*, 2019; Gilleaudeau *et al.*, 2019; Tostevin *et al.*, 2019; Cole *et al.*, 2020; Mänd *et al.*, 2020; Wang *et al.*, 2020); Cr同位素(Frei *et al.*, 2009, 2011, 2013; Crowe *et al.*, 2013; Planavsky *et al.*, 2014b; Cole *et al.*, 2016; Gilleaudeau *et al.*, 2016; Rodler *et al.*, 2016; Babechuk *et al.*, 2017; D'Arcy *et al.*, 2017; Canfield *et al.*, 2018; Gilleaudeau *et al.*, 2018; Huang *et al.*, 2018; Wei *et al.*, 2018a, 2021b; Colwyn *et al.*, 2019; Toma *et al.*, 2019); Tl同位素(Them *et al.*, 2018; Bowman *et al.*, 2019; Ostrander *et al.*, 2019a, 2020; Fan *et al.*, 2020)



开始的时间仍存在较多的争议.造成以上争议的原因可以归结于两个方面:一方面是由于不同氧化还原敏感元素在上地壳中的赋存矿物不同,例如,Mo 主要以硫化物( $\text{MoS}_2$ )形式赋存在上地壳中,而U 主要赋存在长石、辉石、晶质铀矿等矿物中.由于硫化物发生有氧风化作用所需的最低大气氧含量要远小于晶质铀矿发生有氧风化所需的大气氧含量(Rimstidt and Vaughan, 2003),因此不同金属稳定同位素体系所指示的有氧风化作用出现时间存在一定差异.另一方面,由于GOE之前地球表层环境以还原态为主,产氧光合作用生产的氧气会被迅速消耗,从而引起太古宙大气氧含量发生剧烈波动(Anbar and Rouxel, 2007; Ostrander *et al.*, 2021),这可能是导致同种金属稳定同位素在不同时代地层示踪有氧风化作用出现时间存在差异的原因.

**2.1.2 太古宙海水氧化还原状态** 氧化还原敏感金属稳定同位素组成不仅用于限定产氧光合作用起源时间,也在定量评估太古宙海洋的氧化还原状态方面取得重大突破.由于硫化水体环境下的沉积物可以记录海水Mo、Tl同位素组成,硫化环境下沉积的页岩Mo、Tl同位素值被广泛用于恢复古海洋氧化还原状态演化(Nielsen *et al.*, 2011).最近的研究表明,在太古宙末期全球海洋存在完全氧化的大陆架(Ostrander *et al.*, 2019a).研究人员在西澳地区Mt. McRae组地层(2.5 Ga)中发现Mo和Tl同位素存在负相关关系,其中硫化环境下沉积的页岩记录的海水 $\delta^{98}\text{Mo}$ 最高达到1.56‰,  $\epsilon^{205}\text{Tl}$ 也达到-3.57(图4).这指示该时期在海洋中存在着广泛的Mn氧化物的埋藏,而Mn氧化物的埋藏需要水岩界面之下1 m及上覆海水全部氧化.Tl同位素和Mo同位素质量平衡方程模拟结果显示在2.5 Ga时全球海洋氧化水体的面积已达到20%,这表明该时期海洋大陆架区域已完全氧化(Ostrander *et al.*, 2019a).

然而,由于太古宙海洋中 $\text{SO}_4^{2-}$ 浓度极低,海洋硫化水体面积较小,很难形成在硫化环境下沉积的页岩(Reinhard *et al.*, 2009).此外,铁建造的Mo同位素很容易受到Mn氧化物吸附作用的影响,同样无法记录海水Mo同位素信息.研究表明,碳酸盐岩Mo同位素受陆源碎屑组分影响较小,不依赖于硫化水体发育程度或海洋Mo库的大小,因此非骨架碳酸盐岩Mo同位素非常接近其周围海水 $\delta^{98}\text{Mo}$ ,碳酸盐岩Mo同位素已经逐渐成为示踪海水氧化还原变化的新兴指标(Voegelin *et al.*, 2010; Wen *et al.*,

2011; Eroglu *et al.*, 2015; Romaniello *et al.*, 2016; Thoby *et al.*, 2019).对太古宙碳酸盐岩(2.93~2.7 Ga)Mo同位素研究发现,该时期海水 $\delta^{98}\text{Mo}$ 普遍大于1‰.这指示至少在2.93 Ga开始,由Mn氧化物或Fe氧化物吸附作用引起的Mo同位素分馏已经显著改变了海水Mo同位素组成,研究人员推断Mo在氧化环境下的汇在2.7 Ga已经达到较高的比例(Thoby *et al.*, 2019).

## 2.2 大氧化事件(GOE)

GOE引起地球大气中氧气第一次大幅度升高,进而从根本上改变了表生地球元素循环过程和地球的宜居性.沉积地层中硫同位素非质量分馏(mass independent fractionations, MIF)信号的消失被认为是支持GOE存在的最有力证据之一,并将GOE发生的时间限制在2.4~2.2 Ga之间(Farquhar *et al.*, 2000; Bekker *et al.*, 2004; Poulton *et al.*, 2021).此外,对地质历史时期海相沉积物中硫酸盐与黄铁矿硫同位素统计发现,GOE时期硫酸盐与黄铁矿之间的硫同位素组成差异( $\Delta^{34}\text{S} = \delta^{34}\text{S}_{\text{sulfate}} - \delta^{34}\text{S}_{\text{pyrite}}$ )开始逐渐增大,指示该时期大气中氧气含量增加,剧烈的有氧风化使海洋 $\text{SO}_4^{2-}$ 浓度升高(Fike *et al.*, 2015).

相较于传统稳定同位素,目前金属稳定同位素在示踪GOE方面的研究相对较少.最近,Asael *et al.*(2018)通过对2.32~2.06 Ga黑色页岩Mo同位素来重建该时期海洋氧化程度.研究表明,在2.32 Ga由大气氧含量增加引起的强烈有氧风化作用使海洋Mo供应急剧增加,海洋Mo循环处于非稳态,海水Mo同位素剧烈波动.虽然GOE导致大气氧含量永久性升高,但强烈的有氧风化作用造成海洋中氧化还原敏感金属元素循环处于非稳态.同时该时期全球范围内相对缺少碳酸盐岩以及硫化环境下沉积页岩记录,这些都为定量恢复GOE时期海洋氧化程度带来了挑战.

GOE之后的Lomagundi事件(2.22~2.06 Ga)是地质历史持续时间最长的碳同位素正偏事件,对于该事件的成因,传统解释认为与有机碳大量埋藏引起的大气氧含量增加有关,(Lyons *et al.*, 2014; Ossa Ossa *et al.*, 2018a),金属稳定同位素证据支持该时期海洋氧化程度增强.对该时期在硫化环境下形成的页岩沉积物Mo同位素研究结果表明,在Lomagundi碳同位素正偏时期海水 $\delta^{98}\text{Mo}$ 升高但Mo库减小.研究人员推断海洋氧化程度不断增强引起海

水  $\delta^{98}\text{Mo}$  升高,但由于上地壳经历了长时期的有氧风化作用,在 Lomagundi 事件后期硫化物风化效率降低,导致海洋 Mo 库减小 (Asael *et al.*, 2018).

黑色页岩中三价铁与总铁比值 ( $\text{Fe}_2\text{O}_3/\Sigma\text{Fe}_{|\text{Fe}_2\text{O}_3|}$ ) 以及 U 含量的证据支持 Lomagundi 事件结束后大气和海洋氧含量迅速下降 (Bekker and Holland, 2012; Partin *et al.*, 2013). 但是, U 同位素的证据指示该事件结束后海洋氧化程度曾达到现代水平 (Mänd *et al.*, 2020). 研究人员对 Zaonega 组 (~2.0 Ga) 黑色页岩氧化还原敏感元素含量以及 Mo 和 U 同位素进行了测试, 结果发现该沉积地层  $\delta^{238}\text{U}$  最大值达到 +0.79‰ (图 4), 模拟计算结果认为当时海水  $\delta^{238}\text{U}$  已达到现代海水值 (-0.4‰), 这指示在 Lomagundi 事件结束后的几个百万年内海洋仍然保持较高的氧含量 (Mänd *et al.*, 2020).

### 2.3 中元古代大气与海洋氧化还原状态

许多地质证据显示 GOE 之后地球表层环境相对稳定, 生物演化迟缓, 因而被称为枯燥乏味的 10 亿年 (boring billion, 1.8~0.8 Ga) (Large, 2014; Mukherjee *et al.*, 2018). 一部分学者认为中元古代极低的氧气含量阻碍了生物的演化 (Planavsky *et al.*, 2014b), 而另外一部分学者却认为中元古代大气氧含量已经达到相对较高的水平, 生物进化迟缓可能另有原因 (Zhang *et al.*, 2016, 2018d; Canfield *et al.*, 2018). 例如, 生物无机桥假说 (bioinorganic bridge) 认为中元古代广泛发育的硫化水体极大限制了海水中 Mo 的浓度, 由于 Mo 元素是生物固氮酶重要组成元素, 由 Mo 缺乏引起的海洋氮饥荒限制了真核生物的演化 (Anbar and Knoll, 2002). 因此, 对中元古代大气和海洋氧化程度的定量重建是解答以上争论的关键.

目前, 人们对中元古代海洋氧化还原状态的认识仍存在较大争议. 以铁组分为代表的传统地球化学指标研究指示中元古代海洋以缺氧分层为主要特征, 即表层氧化水体、中层硫化水体与深部铁化水体动态共存的分层海洋 (图 1) (Canfield *et al.*, 2008; Poulton *et al.*, 2010; Li *et al.*, 2010; Lyons *et al.*, 2014). 由于  $\text{H}_2\text{S}$  对真核生物具有毒害性, 并且硫化水体会降低许多生命必需元素在海水中的溶解度, 从而阻碍真核生物进化 (Robbins *et al.*, 2016). 因此, 定量恢复中元古代海洋硫化水体面积对于理解该时期真核生物进化缓慢背后的原因具有重要的意义. 而金属稳定同位素不仅可以对中元古代海

洋氧化还原程度进行定量重建, 而且在一定程度上可以限定硫化水体的面积 (Arnold *et al.*, 2004; Kendall *et al.*, 2009, 2011). 通过对古一中元古代硫化背景下沉积的黑色页岩 Mo 同位素分析, 该时期海水平均  $\delta^{98}\text{Mo}$  为 1‰, 质量平衡模型计算结果显示海水中 30%~70% 的 Mo 进入到硫化沉积物中, 为中元古代海洋发育广泛的硫化水体提供了支持 (Arnold *et al.*, 2004; Kendall *et al.*, 2009; Kendall *et al.*, 2011). 然而, 来自碳酸盐岩 U 同位素数据却表明中元古代海洋硫化面积十分有限 (Chen *et al.*, 2018; Tissot *et al.*, 2018; Gilleaudeau *et al.*, 2019). Gilleaudeau *et al.* (2019) 分析了时间跨度从 1.8 Ga 到 0.8 Ga 的碳酸盐岩  $\delta^{238}\text{U}$ , 其平均值为 -0.43‰. 考虑到成岩作用的影响, 推测中元古代海水的  $\delta^{238}\text{U}$  为 -0.73‰~-0.43‰. 结合 U 在海洋中质量平衡循环模型, 他们认为中元古代全球海洋硫化面积不会超过 7%.

尽管不同金属稳定同位素对中元古代硫化水体面积限定结果存在差异, 但不同金属稳定同位素体系都指示中元古代曾发生多次氧化事件 (Diamond *et al.*, 2018; Planavsky *et al.*, 2018; Zhang *et al.*, 2019a). 华北蓟县系高于庄组 (~1.56 Ga) 下部富 Fe-Mn 碳酸盐岩层位 Mo 同位素变化较大且具有较低的  $\delta^{98}\text{Mo}$  值 (可低至 -4.1‰), 这表明该时期海水氧化程度增强, 造成 Fe-Mn 氧化物大量埋藏, 从而对海水 Mo 同位素值造成强烈的影响. 此外, 碳酸盐岩 Mo 同位素表明中元古代早期海水  $\delta^{98}\text{Mo}$  在 0.85‰~1.41‰ 之间, 并通过 Mo 同位素质量平衡模型推测当时海洋氧化面积曾达到 30% (Luo *et al.*, 2021). 同样来自华北克拉通下马岭组 (~1.4 Ga) 黑色页岩的 Mo 同位素和铁组分数据显示, 当时海水  $\delta^{98}\text{Mo}$  曾达到 1.7‰, 高于中元古代海水  $\delta^{98}\text{Mo}$  平均值 (~1.0‰), 指示该时期海洋氧化程度达到比之前更高的水平 (Diamond *et al.*, 2018; Zhang *et al.*, 2019a). 除华北板块外, 在北澳大利亚 McArthur 盆地 1.36 Ga 地层中也观测到中元古代增氧事件信号 (Yang *et al.*, 2017). 该套地层黑色页岩自生成因  $\delta^{238}\text{U}$  平均值为 0.13‰, 在扣除 U 在缺氧环境下的分馏系数 ( $\Delta = 0.60\text{‰} \sim 0.85\text{‰}$ ) 后, Yang *et al.* (2017) 推测 1.36 Ga 时期海水  $\delta^{238}\text{U}$  为 -0.72‰~-0.47‰, 同时 U 同位素质量平衡模型计算结果表明 1.36 Ga 时海洋氧化面积 >75%, 这指示尽管这一时期海水中溶解氧的浓度不会太高, 但深海大部分已经氧化.

然而,相较于中元古代海洋的氧化还原状态的定量重建研究,目前对该时期大气氧含量的定量重建结果争议更大.这方面的认识主要来自Cr同位素的研究.Planavsky *et al.* (2014b)测试了太古宙到显生宙的铁建造和铁岩Cr同位素,结果显示0.8 Ga之前铁建造 $\delta^{53}\text{Cr}$ 接近地壳值,但在此之后 $\delta^{53}\text{Cr}$ 明显升高.这是由于在新元古代之前大气氧含量极低,在有氧风化过程中形成的Mn氧化物有限,无法将 $\text{Cr}^{3+}$ 氧化.研究人员通过Mn氧化物氧化 $\text{Cr}^{3+}$ 热力学过程计算,推测新元古代之前大气氧含量不超过0.1% PAL,认为中元古代大气低氧含量限制了真核藻类的辐射以及后生动物的进化(Planavsky *et al.*, 2014b).之后,Cole *et al.* (2016)统计了自3.5 Ga以来沉积的黑色页岩Cr同位素数据,获得与Planavsky *et al.* (2014b)基本一致的结果.进一步证实了在0.8 Ga之前地球大气氧含量低于0.1% PAL,大陆有氧风化作用较弱.然而,Gilleaudeau *et al.* (2016)和Canfield *et al.* (2018)分别在中元古界碳酸盐岩和黑色页岩地层中发现了较高的 $\delta^{53}\text{Cr}$ 值,最高可达1.77%,据此推测中元古代大气氧含量超过1% PAL,这与之前的研究结果明显不同.Canfield *et al.* (2018)认为在新元古代氧化事件之前大气氧含量已经达到相对较高的水平.

## 2.4 新元古代氧化事件(NOE)

新元古代晚期到寒武纪早期是地质历史中非常特殊的时期,见证了板块构造的剧烈运动、全球气候的急剧变化、海洋碳循环的波动和多细胞真核藻类及后生动物的出现与辐射(图1).许多研究表明新元古代到早寒武世全球海洋的氧化还原条件可能发生了根本性变化,大气和海洋氧含量的增加可能促进了后动植物的起源与快速分化(朱茂炎, 2010; 赵相宽等, 2018; 朱茂炎等, 2019).新元古代氧化事件(NOE)时空演化过程仍充满争议.金属稳定同位素为全面认识NOE时期全球海洋氧化还原状态变化提供了新的视角.

**2.4.1 成冰纪** 新元古代成冰纪经历了地球历史中最严酷的全国性冰期事件,被称为“雪球地球”事件.分子钟与生物标志化合物的证据都表明生物演化在成冰纪经历了重大变革,包括真核藻类的辐射以及后动植物的起源(Love *et al.*, 2009; Brocks *et al.*, 2017; Hoshino *et al.*, 2017).重建成冰纪全球海洋氧化还原状态对理解“雪球地球”事件与生命演化之间的内在成因联系具有重要科学意义.华南

成冰系大塘坡组(660~650 Ma)黑色页岩Mo同位素测试结果表明该时期海水 $\delta^{98}\text{Mo}$ 约为1‰,海洋仍处于广泛缺氧状态(Cheng *et al.*, 2018; Tan *et al.*, 2021).与Mo同位素反映的雪球地球间冰期海洋保持高度缺氧状态不同的是,U同位素研究认为在Sturtian冰期解体之后,海洋曾发生一次短暂的氧化事件(Lau *et al.*, 2017).Lau *et al.* (2017)分析了蒙古国Taishir组两个灰岩剖面 $\delta^{238}\text{U}$ ,结果显示Sturtian冰碛岩之上的灰岩样品 $\delta^{238}\text{U}$ 相对较高,平均值为-0.47‰,略小于现代海水 $\delta^{238}\text{U}$ (-0.39‰),指示当时海洋具有相对较高的氧化面积.之后 $\delta^{238}\text{U}$ 下降了0.3‰,结合同步负偏的 $\delta^{13}\text{C}$ 值,Lau *et al.* (2017)认为海洋在短暂氧化之后,海洋表层大量的有机碳再矿化消耗水体中的氧气,使缺氧面积增大.然而,Wei *et al.* (2021a)却认为如果考虑成岩作用对碳酸盐岩U同位素的影响,成冰纪间冰期海水 $\delta^{238}\text{U}$ 要远小于现代海水值,成冰纪海洋应该以缺氧(或硫化)为主,但是会出现亚氧化或铁化水体的扩张.

**2.4.2 埃迪卡拉纪** 传统的地球化学指标,如氧化还原敏感元素富集程度(RSTE)、铁组分、硫同位素以及氮同位素研究均表明埃迪卡拉纪海洋曾发生多次氧化事件(Sahoo *et al.*, 2012, 2016; Shi *et al.*, 2018; Wang *et al.*, 2018).最近,Mo、Tl、U同位素的研究指示埃迪卡拉纪海洋氧化程度曾接近现代水平.

研究人员在华南埃迪卡拉系陡山沱组多条斜坡相以及深水相剖面(九龙湾、五河、桃映、袁家、榕溪)都发现了较低的Mo同位素值( $< -2\text{‰}$ ),且剖面 $\delta^{98}\text{Mo}$ 存在多次负偏波动(Chen *et al.*, 2015; Ostrander *et al.*, 2019b; Ye *et al.*, 2020).他们将这种较低 $\delta^{98}\text{Mo}$ 值归因于海洋中弱硫化水体的扩张或者Fe-Mn搬运机作用的发育.但无论是弱硫化水体的扩张还是Fe-Mn搬运机作用的发育都指示该时期海洋氧化程度增强,使斜坡相和部分深水相沉积物多次处于氧化或亚氧化环境中,为埃迪卡拉纪多次增氧事件提供了证据(Ostrander *et al.*, 2019b).此外,华南埃迪卡拉系陡山沱组四段顶部黑色页岩 $\delta^{98}\text{Mo}$ 曾达到+2.08‰,接近现代海水Mo同位素值( $\delta^{98}\text{Mo}=2.34\text{‰}$ ).这指示海洋氧化程度在新元古代晚期第一次接近现代水平,打破了自GOE以来全球海洋以大面积缺氧为主的状态(Kendall *et al.*, 2015).该层位U同位素研究也指示这一时期海水 $\delta^{238}\text{U}$ 不断升高,为埃迪卡拉纪末期海水氧化程度增

强提供了新的证据(Kendall *et al.*, 2015).

Tl 同位素同样捕捉到新元古代多次氧化事件, Ostrander *et al.* (2020) 在扬子板块新元古代陡山沱组 RSTE 富集层位发现  $\epsilon^{205}\text{Tl}$  同步负偏, 这与前人提出的新元古代脉冲式增氧事件一致(Sahoo *et al.*, 2016). 同时 Fan *et al.* (2020) 发现新元古代“Shuram”碳同位素负偏事件期间海水平均  $\epsilon^{205}\text{Tl}$  为 -6, 这与现代海水  $\epsilon^{205}\text{Tl}$  值一致, 表明新元古代晚期全球海洋氧化程度达到现今水平.

相较于地质历史其他时期, 新元古代晚期至早寒武世积累了最丰富的 U 同位素数据(图 4). 在全球已经建立起来的高分辨率地层框架基础上, 埃迪卡拉纪全球海水  $\delta^{238}\text{U}$  整体呈现逐渐升高趋势, 并在埃迪卡拉纪结束时达到现代海水值. 同时  $\delta^{238}\text{U}$  存在多次负偏波动, 这表明尽管埃迪卡拉纪海洋逐渐氧化, 但同时也存在多次缺氧事件(Kendall *et al.*, 2015; Wei *et al.*, 2018a, 2021a; Zhang *et al.*, 2018c, 2019b; Tostevin *et al.*, 2019; Cao *et al.*, 2020; Li *et al.*, 2020)(图 4). Wei *et al.* (2021a) 分析了华南九龙湾剖面陡山沱组二段(635~570 Ma)碳酸盐岩 U 同位素数据, 结果显示埃迪卡拉纪早期海水平均  $\delta^{238}\text{U}$  为  $-0.66\text{‰} \pm 0.04\text{‰}$ , 这表明埃迪卡拉纪早期海洋氧化程度虽然相较于成冰纪有所增强, 但仍然以缺氧状态为主. 陡山沱组三段记录的“Shuram”负偏事件是地质历史时期负偏程度最大的碳同位素负偏事件, 持续时间长达 10 Ma (570~560 Ma) (Rooney *et al.*, 2020). 对该阶段碳酸盐岩 U 同位素数据研究表明“Shuram”负偏时期海水  $\delta^{238}\text{U}$  增加到了相对较高的水平, 即使在扣除成岩作用对碳酸盐岩 U 同位素影响后, 部分碳酸盐岩  $\delta^{238}\text{U}$  仍超过了现代海水值. 通过 U 同位素质量平衡模型计算出“Shuram”负偏时期海洋氧化面积接近 100%, 表明此时全球海洋氧化程度接近现代水平(Zhang *et al.*, 2019b; Cao *et al.*, 2020).

**2.4.3 早寒武世** 针对寒武纪早期海洋氧化还原状态与寒武纪生命大爆发之间的联系, 研究人员利用金属稳定同位素进行了大量的研究. 铁组分研究结果表明扬子板块早寒武世黑色页岩广泛形成于强硫化环境中, 为恢复该时期海水 Mo 同位素提供了良好的研究载体(Wille *et al.*, 2008; Wen *et al.*, 2011, 2015; Xu *et al.*, 2012; Chen *et al.*, 2015; Cheng *et al.*, 2017; Yin *et al.*, 2018; Dong *et al.*, 2019; Ye *et al.*, 2020). 在扬子板块下寒武统高精度地层年代

对比框架下, 这些 Mo 同位素数据都表现出一个共同的特点, 即寒武纪生命大爆发前夕, 寒武系第二阶和第三阶交界处, 沉积物  $\delta^{98}\text{Mo}$  首次达到现代水平( $\delta^{98}\text{Mo} = 2.34\text{‰}$ ) (Chen *et al.*, 2015; Wen *et al.*, 2015; Cheng *et al.*, 2017). Chen *et al.* (2015) 根据海洋 Mo 循环的同位素质量守恒关系推测在 521 Ma 时海洋中强氧化和适度氧化面积超过 97%, 海洋氧化程度在寒武纪早期时期达到现代水平.

U 同位素证据同样支持早寒武世海水氧化程度增强促进了后生动物的辐射与发展. 在经历埃迪卡拉纪末期海洋缺氧之后, 海洋  $\delta^{238}\text{U}$  值逐渐升高, 最终在 541 Ma 时达到现代海水值( $-0.39\text{‰}$ ), 这指示此时海洋氧化程度接近现代水平(Wei *et al.*, 2018b). 但在早寒武世幸运期末期(529 Ma)以及第二期中期(526 Ma)海洋经历了两次缺氧事件(Wei *et al.*, 2018a; Dahl *et al.*, 2019). 基于早寒武世海洋氧化还原状态动态波动模式, Wei *et al.* (2018a) 认为该时期海洋脉冲式的缺氧事件使生物栖息地碎片化, 造成早期生态系统不稳定, 从而促进了后生物辐射以及形态多样化.

### 3 总结与展望

综上所述, 利用金属稳定同位素重建深时地球大气与海洋氧化程度目前取得主要进展如下: (1) Mo、U、Cr 同位素通过示踪有氧风化作用将产氧光合作用起源时间限制在 3.0 Ga, 但这一结果仍存在争议. Mo 和 Tl 同位素则指示太古宙末期全球海洋曾达到较高的氧化程度, 浅海大陆架区域已经完全氧化; (2) 对 GOE 时期海水 Mo 同位素研究表明, 由大气氧含量升高带来的强烈有氧风化作用使该时期海洋 Mo 循环处于非稳态, 导致海水 Mo 同位素剧烈波动. U 同位素证据表明, Lomagundi 事件时期以及该事件结束后的几个百万年内, 全球海洋氧化程度持续保持在较高的水平; (3) 不同金属稳定同位素对中元古代海洋硫化水体面积限定结果目前存在差异, Mo 同位素证据支持海洋发育广泛的硫化水体, 但 U 同位素却表明中元古代全球海洋硫化面积十分有限. 然而, Mo、U 同位素都记录了以缺氧为主导的中元古代海洋曾发生多次增氧事件, 为真核生物演化提供了能量基础. 对于该时期大气氧含量的争议则需要对该阶段的地层开展更多 Cr 同位素研究工作; (4) Mo、U、Tl 同位素都记录了埃迪卡拉纪海洋曾发生多次增氧事件, 并指示在早寒武世大

气与海洋的氧化程度达到现今的水平。

尽管 Mo、U、Tl、Cr 等氧化还原敏感金属稳定同位素在示踪地球增氧历程方面已经取得较大的进展,但在应用过程中仍存在以下几方面的问题亟待解决。(1)由于前寒武纪海洋中氧化还原敏感金属元素的储库和同位素组成与现代海洋存在差别,对现代海洋氧化还原状态的评估阈值应用于古代海洋存在许多不确定性。特别是利用 Mo、U 同位素质量平衡方程来定量恢复地质历史时期海水氧化、硫化以及铁化水体面积时,海水 Mo、U 元素循环通量变化和区域氧化还原条件都会对结果产生重要影响 (Partin *et al.*, 2013; Reinhard *et al.*, 2013); (2) 许多太古宇和元古宇碳酸盐岩具有与地壳和河流输入相似  $\delta^{238}\text{U}$  值(图 4),并未表现出明显的 U 同位素分馏。这与基于 U 同位素分馏原理认为在太古代和元古代缺氧海洋中海水和碳酸盐岩具有较低的  $\delta^{238}\text{U}$  值的认识不一致。这对利用 U 同位素定量重建前寒武纪海洋氧化还原状态提出了巨大的挑战 (Cole *et al.*, 2020; Lau *et al.*, 2020); (3) 对 U、Tl、Cr 同位素在缺氧环境下分馏机制的认识仍然存在争议,特别是非硫化缺氧环境下的分馏系数还未得到很好的限定。此外,对碳酸盐岩成岩过程中 U 和 Cr 同位素分馏机制的研究仍然不足; (4) 目前对 Tl 和 Cr 同位素在现代全球海洋中的循环过程以及各地质储库同位素组成的研究相对较少,这阻碍了利用 Tl、Cr 同位素重建地质历史时期海水氧化还原状态变化。

由于氧化还原敏感金属同位素体系发生分馏的  $p\text{O}_2$  阈值较低,被广泛用于重建前寒武纪大气与海洋氧化还原状态。然而,不同的金属稳定同位素在氧化还原条件变化时分馏方向和分馏程度存在差异,导致不同研究重建的结果往往存在一定差异。因此,我们建议,对同一地层采用多指标结合的方法来综合研究,同时结合同时期全球其他地区的数据可以约束区域或全球海洋氧化还原状态变化。例如,Mo 同位素和 U 同位素联合可以限定水体中硫化区域与非硫化区域的面积; Mo 同位素和 Tl 同位素结合可以更好的制约缺氧水体与氧化水体的面积。此外,应加强对具有不同氧化还原敏感度的新兴金属稳定同位素体系测试方法和分馏机理的研究,例如 Ce、Sb、V、Re 等稳定同位素,为更全面地认识深时地球增氧过程提供新的手段。除此之外,越来越多的研究表明,地质历史时期地球增氧事件与

深部过程有着紧密的联系 (Lee *et al.*, 2016; Kadoya *et al.*, 2020)。未来我们应加强金属稳定同位素在示踪地球内部活动及其地表环境响应方面的研究。

致谢:文章撰写阶段得到了中科院地质与地球物理研究所周锡强老师和西北大学地质学系马龙老师的帮助,在此致以诚挚的感谢;感谢两位匿名审稿人提出的建设性意见。

## References

- Ahmad, Q., Wille, M., König, S., et al., 2021. The Molybdenum Isotope Subduction Recycling Conundrum: A Case Study from the Tongan Subduction Zone, Western Alps and Alpine Corsica. *Chemical Geology*, 576: 120231. <https://doi.org/10.1016/j.chemgeo.2021.120231>
- Albut, G., Babechuk, M. G., Kleinhanns, I. C., et al., 2018. Modern rather than Mesoarchaeon Oxidative Weathering Responsible for the Heavy Stable Cr Isotopic Signatures of the 2.95 Ga Old Ijzermijn Iron Formation (South Africa). *Geochimica et Cosmochimica Acta*, 228: 157–189. <https://doi.org/10.1016/j.gca.2018.02.034>
- Algeo, T. J., Li, C., 2020. Redox Classification and Calibration of Redox Thresholds in Sedimentary Systems. *Geochimica et Cosmochimica Acta*, 287: 8–26. <https://doi.org/10.1016/j.gca.2020.01.055>
- Allwood, A. C., Walter, M. R., Kamber, B. S., et al., 2006. Stromatolite Reef from the Early Archaean Era of Australia. *Nature*, 441: 714–718. <https://doi.org/10.1038/nature04764>
- Anbar, A. D., Knoll, A. H., 2002. Proterozoic Ocean Chemistry and Evolution: A Bioinorganic Bridge? *Science*, 297 (5584): 1137–1142. <https://doi.org/10.1126/science.1069651>
- Anbar, A. D., Rouxel, O., 2007. Metal Stable Isotopes in Paleooceanography. *Annual Review of Earth and Planetary Sciences*, 35(1): 717–746. <https://doi.org/10.1146/annurev.earth.34.031405.125029>
- Anders, E., Grevesse, N., 1989. Abundances of the Elements: Meteoritic and Solar. *Geochimica et Cosmochimica Acta*, 53(1): 197–214. [https://doi.org/10.1016/0016-7037\(89\)90286-x](https://doi.org/10.1016/0016-7037(89)90286-x)
- Andersen, M. B., Elliott, T., Freymuth, H., et al., 2015. The Terrestrial Uranium Isotope Cycle. *Nature*, 517: 356–359. <https://doi.org/10.1038/nature14062>
- Andersen, M. B., Matthews, A., Vance, D., et al., 2018. A 10-Fold Decline in the Deep Eastern Mediterranean Thermohaline Overturning Circulation during the Last Interglacial Period. *Earth and Planetary Science Letters*, 503:

- 58–67. <https://doi.org/10.1016/j.epsl.2018.09.013>
- Andersen, M. B., Romaniello, S., Vance, D., et al., 2014. A Modern Framework for the Interpretation of  $^{238}\text{U}/^{235}\text{U}$  in Studies of Ancient Ocean Redox. *Earth and Planetary Science Letters*, 400: 184–194. <https://doi.org/10.1016/j.epsl.2014.05.051>
- Andersen, M. B., Stirling, C. H., Weyer, S., 2017. Uranium Isotope Fractionation. *Reviews in Mineralogy and Geochemistry*, 82(1): 799–850. <https://doi.org/10.2138/rmg.2017.82.19>
- Andersen, M. B., Vance, D., Morford, J. L., et al., 2016. Closing in on the Marine  $^{238}\text{U}/^{235}\text{U}$  Budget. *Chemical Geology*, 420: 11–22. <https://doi.org/10.1016/j.chemgeo.2015.10.041>
- Archer, C., Vance, D., 2008. The Isotopic Signature of the Global Riverine Molybdenum Flux and Anoxia in the Ancient Oceans. *Nature Geoscience*, 1(9): 597–600. <https://doi.org/10.1038/ngeo282>
- Arnold, G. L., Anbar, A., Barling, J., et al., 2004. Molybdenum Isotope Evidence for Widespread Anoxia in Mid-Proterozoic Oceans. *Science*, 304(5667): 87–90. <https://doi.org/10.1126/science.1091785>
- Asael, D., Rouxel, O., Poulton, S. W., et al., 2018. Molybdenum Record from Black Shales Indicates Oscillating Atmospheric Oxygen Levels in the Early Paleoproterozoic. *American Journal of Science*, 318(3): 275–299. <https://doi.org/10.2475/03.2018.01>
- Asael, D., Tissot, F. L. H., Reinhard, C. T., et al., 2013. Coupled Molybdenum, Iron and Uranium Stable Isotopes as Oceanic Paleoredox Proxies during the Paleoproterozoic Shunga Event. *Chemical Geology*, 362: 193–210. <https://doi.org/10.1016/j.chemgeo.2013.08.003>
- Babechuk, M. G., Kleinhans, I. C., Schoenberg, R., 2017. Chromium Geochemistry of the ca. 1.85 Ga Flin Flon Paleosol. *Geobiology*, 15(1): 30–50. <https://doi.org/10.1111/gbi.12203>
- Barling, J., Arnold, G. L., Anbar, A. D., 2001. Natural Mass-Dependent Variations in the Isotopic Composition of Molybdenum. *Earth and Planetary Science Letters*, 193(3–4): 447–457. [https://doi.org/10.1016/s0012-821x\(01\)00514-3](https://doi.org/10.1016/s0012-821x(01)00514-3)
- Bartlett, R., Elrick, M., Wheeley, J. R., et al., 2018. Abrupt Global-Ocean Anoxia during the Late Ordovician-Early Silurian Detected Using Uranium Isotopes of Marine Carbonates. *Proceedings of the National Academy of Sciences*, 115(23): 5896–5901. <https://doi.org/10.1073/pnas.1802438115>
- Bekker, A., Holland, H. D., 2012. Oxygen Overshoot and Recovery during the Early Paleoproterozoic. *Earth and Planetary Science Letters*, 317–318: 295–304. <https://doi.org/10.1016/j.epsl.2011.12.012>
- Bekker, A., Holland, H. D., Wang, P. L., et al., 2004. Dating the Rise of Atmospheric Oxygen. *Nature*, 427: 117–120. <https://doi.org/10.1038/nature02260>
- Bowman, C. N., Young, S. A., Kaljo, D., et al., 2019. Linking the Progressive Expansion of Reducing Conditions to a Stepwise Mass Extinction Event in the Late Silurian Oceans. *Geology*, 47(10): 968–972. <https://doi.org/10.1130/g46571.1>
- Brennecke, G. A., Herrmann, A. D., Algeo, T. J., et al., 2011. Rapid Expansion of Oceanic Anoxia Immediately before the End-Permian Mass Extinction. *Proceedings of the National Academy of Sciences of the United States of America*, 108(43): 17631–17634. <https://doi.org/10.1073/pnas.1106039108>
- Brocks, J. J., Jarrett, A. J. M., Sirantoine, E., et al., 2017. The Rise of Algae in Cryogenian Oceans and the Emergence of Animals. *Nature*, 548: 578–581. <https://doi.org/10.1038/nature23457>
- Brown, S. T., Basu, A., Ding, X., et al., 2018. Uranium Isotope Fractionation by Abiotic Reductive Precipitation. *Proceedings of the National Academy of Sciences*, 115(35): 8688–8693. <https://doi.org/10.1073/pnas.1805234115>
- Brüske, A., Martin, A. N., Rammensee, P., et al., 2020. The Onset of Oxidative Weathering Traced by Uranium Isotopes. *Precambrian Research*, 338: 105583. <https://doi.org/10.1016/j.precamres.2019.105583>
- Canfield, D. E., Poulton, S. W., Knoll, A. H., et al., 2008. Ferruginous Conditions Dominated Later Neoproterozoic Deep-Water Chemistry. *Science*, 321(5891): 949–952. <https://doi.org/10.1126/science.1154499>
- Canfield, D. E., Thamdrup, B., 2009. Towards a Consistent Classification Scheme for Geochemical Environments, or, Why We Wish the Term ‘Suboxic’ would Go away. *Geobiology*, 7(4): 385–392. <https://doi.org/10.1111/j.1472-4669.2009.00214.x>
- Canfield, D. E., Zhang, S. C., Frank, A. B., et al., 2018. Highly Fractionated Chromium Isotopes in Mesoproterozoic-Aged Shales and Atmospheric Oxygen. *Nature Communications*, 9: 2871. <https://doi.org/10.1038/s41467-018-05263-9>
- Cao, M. C., Daines, S. J., Lenton, T. M., et al., 2020. Comparison of Ediacaran Platform and Slope  $\delta^{238}\text{U}$  Records in South China: Implications for Global-Ocean Oxygenation

- and the Origin of the Shuram Excursion. *Geochimica et Cosmochimica Acta*, 287: 111–124. <https://doi.org/10.1016/j.gca.2020.04.035>
- Catling, D. C., Zahnle, K. J., McKay, C. P., 2001. Biogenic Methane, Hydrogen Escape, and the Irreversible Oxidation of Early Earth. *Science*, 293(5531):839–843. <https://doi.org/10.1126/science.1061976>
- Chen, X., Ling, H.F., Vance, D., et al., 2015. Rise to Modern Levels of Ocean Oxygenation Coincided with the Cambrian Radiation of Animals. *Nature Communications*, 6: 7142. <https://doi.org/10.1038/ncomms8142>
- Chen, X.M., Romaniello, S.J., Herrmann, A.D., et al., 2018. Diagenetic Effects on Uranium Isotope Fractionation in Carbonate Sediments from the Bahamas. *Geochimica et Cosmochimica Acta*, 237: 294–311. <https://doi.org/10.1016/j.gca.2018.06.026>
- Cheng, M., Li, C., Chen, X., et al., 2018. Delayed Neoproterozoic Oceanic Oxygenation: Evidence from Mo Isotopes of the Cryogenian Datangpo Formation. *Precambrian Research*, 319: 187–197. <https://doi.org/10.1016/j.precamres.2017.12.007>
- Cheng, M., Li, C., Zhou, L., et al., 2015. Mo Marine Geochemistry and Reconstruction of Ancient Ocean Redox States. *Scientia Sinica(Terrae)*, 45(11):1649–1660(in Chinese).
- Cheng, M., Li, C., Zhou, L., et al., 2016. Marine Mo Biogeochemistry in the Context of Dynamically Euxinic Mid-Depth Waters: A Case Study of the Lower Cambrian Niutitang Shales, South China. *Geochimica et Cosmochimica Acta*, 183: 79–93. <https://doi.org/10.1016/j.gca.2016.03.035>
- Cheng, M., Li, C., Zhou, L., et al., 2017. Transient Deep-Water Oxygenation in the Early Cambrian Nanhua Basin, South China. *Geochimica et Cosmochimica Acta*, 210:42–58. <https://doi.org/10.1016/j.gca.2017.04.032>
- Cole, D.B., Planavsky, N.J., Longley, M., et al., 2020. Uranium Isotope Fractionation in Non-Sulfidic Anoxic Settings and the Global Uranium Isotope Mass Balance. *Global Biogeochemical Cycles*, 34(8): e2020gb006649. <https://doi.org/10.1029/2020gb006649>
- Cole, D.B., Reinhard, C.T., Wang, X.L., et al., 2016. A Shale-Hosted Cr Isotope Record of Low Atmospheric Oxygen during the Proterozoic. *Geology*, 44(7):555–558. <https://doi.org/10.1130/g37787.1>
- Collier, R. W., 1985. Molybdenum in the Northeast Pacific Ocean. *Limnology and Oceanography*, 30(6): 1351–1354. <https://doi.org/10.4319/lo.1985.30.6.1351>
- Colwyn, D.A., Sheldon, N.D., Maynard, J.B., et al., 2019. A Paleosol Record of the Evolution of Cr Redox Cycling and Evidence for an Increase in Atmospheric Oxygen during the Neoproterozoic. *Geobiology*, 17(6): 579–593. <https://doi.org/10.1111/gbi.12360>
- Crowe, S.A., Døssing, L.N., Beukes, N.J., et al., 2013. Atmospheric Oxygenation Three Billion Years Ago. *Nature*, 501:535–538. <https://doi.org/10.1038/nature12426>
- D'Arcy, J., Gilleaudeau, G.J., Peralta, S., et al., 2017. Redox Fluctuations in the Early Ordovician Oceans: An Insight from Chromium Stable Isotopes. *Chemical Geology*, 448: 1–12. <https://doi.org/10.1016/j.chemgeo.2016.10.012>
- Dahl, T.W., Boyle, R.A., Canfield, D.E., et al., 2014. Uranium Isotopes Distinguish Two Geochemically Distinct Stages during the Later Cambrian SPICE Event. *Earth and Planetary Science Letters*, 401: 313–326. <https://doi.org/10.1016/j.epsl.2014.05.043>
- Dahl, T.W., Canfield, D.E., Rosing, M.T., et al., 2011. Molybdenum Evidence for Expansive Sulfidic Water Masses in ~750 Ma Oceans. *Earth and Planetary Science Letters*, 311(3–4): 264–274. <https://doi.org/10.1016/j.epsl.2011.09.016>
- Dahl, T.W., Connelly, J.N., Li, D., et al., 2019. Atmosphere-Ocean Oxygen and Productivity Dynamics during Early Animal Radiations. *Proceedings of the National Academy of Sciences of the United States of America*, 116(39): 19352–19361. <https://doi.org/10.1073/pnas.1901178116>
- Diamond, C.W., Planavsky, N.J., Wang, C., et al., 2018. What the ~1.4 Ga Xiamaling Formation can and cannot Tell Us about the Mid-Proterozoic Ocean. *Geobiology*, 16(3): 219–236. <https://doi.org/10.1111/gbi.12282>
- Dickson, A.J., Cohen, A.S., Coe, A.L., 2012. Seawater Oxygenation during the Paleocene-Eocene Thermal Maximum. *Geology*, 40(7): 639–642. <https://doi.org/10.1130/g32977.1>
- Dong, B.H., Long, X.P., Li, J., et al., 2019. Mo Isotopic Variations of a Cambrian Sedimentary Profile in the Huangling Area, South China: Evidence for Redox Environment Corresponding to the Cambrian Explosion. *Gondwana Research*, 69: 45–55. <https://doi.org/10.1016/j.gr.2018.12.002>
- Duan, Y., Anbar, A.D., Arnold, G.L., et al., 2010. Molybdenum Isotope Evidence for Mild Environmental Oxygenation before the Great Oxidation Event. *Geochimica et Cosmochimica Acta*, 74(23): 6655–6668. <https://doi.org/10.1016/j.gca.2010.08.035>
- Dunk, R.M., Mills, R.A., Jenkins, W.J., 2002. A Reevaluation

- of the Oceanic Uranium Budget for the Holocene. *Chemical Geology*, 190(1–4): 45–67. [https://doi.org/10.1016/s0009-2541\(02\)00110-9](https://doi.org/10.1016/s0009-2541(02)00110-9)
- Eary, L. E., Rai, D., 1987. Kinetics of Chromium (III) Oxidation to Chromium (VI) by Reaction with Manganese Dioxide. *Environmental Science & Technology*, 21(12): 1187–1193. <https://doi.org/10.1021/es00165a005>
- Elrick, M., Polyak, V., Algeo, T. J., et al., 2017. Global-Ocean Redox Variation during the Middle - Late Permian through Early Triassic Based on Uranium Isotope and Th/U Trends of Marine Carbonates. *Geology*, 45(2): 163–166. <https://doi.org/10.1130/g38585.1>
- Erickson, B. E., Helz, G. R., 2000. Molybdenum (VI) Speciation in Sulfidic Waters: Stability and Lability of Thiomolybdates. *Geochimica et Cosmochimica Acta*, 64(7): 1149–1158. [https://doi.org/10.1016/s0016-7037\(99\)00423-8](https://doi.org/10.1016/s0016-7037(99)00423-8)
- Eroglu, S., Schoenberg, R., Wille, M., et al., 2015. Geochemical Stratigraphy, Sedimentology, and Mo Isotope Systematics of the ca. 2.58–2.50 Ga-Old Transvaal Supergroup Carbonate Platform, South Africa. *Precambrian Research*, 266: 27–46. <https://doi.org/10.1016/j.precamres.2015.04.014>
- Erwin, D. H., Laflamme, M., Tweedt, S. M., et al., 2011. The Cambrian Conundrum: Early Divergence and Later Ecological Success in the Early History of Animals. *Science*, 334(6059): 1091–1097. <https://doi.org/10.1126/science.1206375>
- Fan, H. F., Nielsen, S. G., Owens, J. D., et al., 2020. Constraining Oceanic Oxygenation during the Shuram Excursion in South China Using Thallium Isotopes. *Geobiology*, 18(3): 348–365. <https://doi.org/10.1111/gbi.12379>
- Farquhar, J., Bao, H. M., Thiemens, M., 2000. Atmospheric Influence of Earth's Earliest Sulfur Cycle. *Science*, 289(5480): 756–758. <https://doi.org/10.1126/science.289.5480.756>
- Fendorf, S. E., Fendorf, M., Sparks, D. L., et al., 1992. Inhibitory Mechanisms of Cr(III) Oxidation by  $\delta$ -MnO<sub>2</sub>. *Journal of Colloid and Interface Science*, 153(1): 37–54. [https://doi.org/10.1016/0021-9797\(92\)90296-x](https://doi.org/10.1016/0021-9797(92)90296-x)
- Fike, D. A., Bradley, A. S., Rose, C. V., 2015. Rethinking the Ancient Sulfur Cycle. *Annual Review of Earth and Planetary Sciences*, 43(1): 593–622. <https://doi.org/10.1146/annurev-earth-060313-054802>
- Fike, D. A., Grotzinger, J. P., 2008. A Paired Sulfate-Pyrite  $\delta^{34}\text{S}$  Approach to Understanding the Evolution of the Ediacaran-Cambrian Sulfur Cycle. *Geochimica et Cosmochimica Acta*, 72(11): 2636–2648. <https://doi.org/10.1016/j.gca.2008.03.021>
- Fischer, W. W., Hemp, J., Johnson, J. E., 2016. Evolution of Oxygenic Photosynthesis. *Annual Review of Earth and Planetary Sciences*, 44(1): 647–683. <https://doi.org/10.1146/annurev-earth-060313-054810>
- Frei, R., Gaucher, C., Døssing, L. N., et al., 2011. Chromium Isotopes in Carbonates: A Tracer for Climate Change and for Reconstructing the Redox State of Ancient Seawater. *Earth and Planetary Science Letters*, 312(1–2): 114–125. <https://doi.org/10.1016/j.epsl.2011.10.009>
- Frei, R., Gaucher, C., Poulton, S. W., et al., 2009. Fluctuations in Precambrian Atmospheric Oxygenation Recorded by Chromium Isotopes. *Nature*, 461: 250–253. <https://doi.org/10.1038/nature08266>
- Frei, R., Gaucher, C., Stolper, D., et al., 2013. Fluctuations in Late Neoproterozoic Atmospheric Oxidation-Cr Isotope Chemostratigraphy and Iron Speciation of the Late Ediacaran Lower Arroyo Del Soldado Group (Uruguay). *Gondwana Research*, 23(2): 797–811. <https://doi.org/10.1016/j.gr.2012.06.004>
- Gilleaudeau, G. J., Frei, R., Kaufman, A. J., et al., 2016. Oxygenation of the Mid-Proterozoic Atmosphere: Clues from Chromium Isotopes in Carbonates. *Geochemical Perspectives Letters*, 178–187. <https://doi.org/10.7185/geochemlet.1618>
- Gilleaudeau, G. J., Romaniello, S. J., Luo, G. M., et al., 2019. Uranium Isotope Evidence for Limited Euxinia in Mid-Proterozoic Oceans. *Earth and Planetary Science Letters*, 521: 150–157. <https://doi.org/10.1016/j.epsl.2019.06.012>
- Gilleaudeau, G. J., Sahoo, S. K., Ostrander, C. M., et al., 2020. Molybdenum Isotope and Trace Metal Signals in an Iron-Rich Mesoproterozoic Ocean: A Snapshot from the Vindhyan Basin, India. *Precambrian Research*, 343: 105718. <https://doi.org/10.1016/j.precamres.2020.105718>
- Gilleaudeau, G. J., Voegelin, A. R., Thibault, N., et al., 2018. Stable Isotope Records across the Cretaceous-Paleogene Transition, Stevns Klint, Denmark: New Insights from the Chromium Isotope System. *Geochimica et Cosmochimica Acta*, 235: 305–332. <https://doi.org/10.1016/j.gca.2018.04.028>
- Goldberg, T., Archer, C., Vance, D., et al., 2012. Controls on Mo Isotope Fractionations in a Mn-Rich Anoxic Marine Sediment, Gullmar Fjord, Sweden. *Chemical Geology*, 296–297: 73–82. <https://doi.org/10.1016/j.chemgeo.2011.12.020>



- Gordon, G.W., Lyons, T.W., Arnold, G.L., et al., 2009. When do Black Shales Tell Molybdenum Isotope Tales? *Geology*, 37(6):535–538. <https://doi.org/10.1130/g25186a.1>
- Goring-Harford, H.J., Klar, J.K., Pearce, C.R., et al., 2018. Behaviour of Chromium Isotopes in the Eastern Sub-Tropical Atlantic Oxygen Minimum Zone. *Geochimica et Cosmochimica Acta*, 236:41–59. <https://doi.org/10.1016/j.gca.2018.03.004>
- Greaney, A.T., Rudnick, R.L., Romaniello, S.J., et al., 2020. Molybdenum Isotope Fractionation in Glacial Diamictites Tracks the Onset of Oxidative Weathering of the Continental Crust. *Earth and Planetary Science Letters*, 534:116083. <https://doi.org/10.1016/j.epsl.2020.116083>
- Gueguen, B., Reinhard, C.T., Algeo, T.J., et al., 2016. The Chromium Isotope Composition of Reducing and Oxidizing Marine Sediments. *Geochimica et Cosmochimica Acta*, 184:1–19. <https://doi.org/10.1016/j.gca.2016.04.004>
- Herrmann, A.D., Kendall, B., Algeo, T.J., et al., 2012. Anomalous Molybdenum Isotope Trends in Upper Pennsylvanian Euxinic Facies: Significance for Use of  $\delta^{98}\text{Mo}$  as a Global Marine Redox Proxy. *Chemical Geology*, 324–325: 87–98. <https://doi.org/10.1016/j.chemgeo.2012.05.013>
- Hinojosa, J.L., Stirling, C.H., Reid, M.R., et al., 2016. Trace Metal Cycling and  $^{238}\text{U}/^{235}\text{U}$  in New Zealand's Fjords: Implications for Reconstructing Global Paleoredox Conditions in Organic-Rich Sediments. *Geochimica et Cosmochimica Acta*, 179: 89–109. <https://doi.org/10.1016/j.gca.2016.02.006>
- Holland, H.D., 2006. The Oxygenation of the Atmosphere and Oceans. *Philosophical Transactions of the Royal Society of London Series B, Biological Sciences*, 361(1470): 903–915. <https://doi.org/10.1098/rstb.2006.1838>
- Holland, H.D., 2007. The Geologic History of Seawater. Treatise on Geochemistry. Elsevier, Amsterdam. <https://doi.org/10.1016/b0-08-043751-6/06122-3>
- Holmden, C., Amini, M., Francois, R., 2015. Uranium Isotope Fractionation in Saanich Inlet: A Modern Analog Study of a Paleoredox Tracer. *Geochimica et Cosmochimica Acta*, 153: 202–215. <https://doi.org/10.1016/j.gca.2014.11.012>
- Hood, A.V.S., Planavsky, N.J., Wallace, M.W., et al., 2016. Integrated Geochemical - Petrographic Insights from Component-Selective  $\delta^{238}\text{U}$  of Cryogenian Marine Carbonates. *Geology*, 44(11): 935–938. <https://doi.org/10.1130/g38533.1>
- Hoshino, Y., Poshibaeva, A., Meredith, W., et al., 2017. Cryogenian Evolution of Stigmasteroid Biosynthesis. *Science Advances*, 3(9): e1700887. <https://doi.org/10.1126/sciadv.1700887>
- Huang, J., Liu, J., Zhang, Y.N., et al., 2018. Cr Isotopic Composition of the Laobao Cherts during the Ediacaran - Cambrian Transition in South China. *Chemical Geology*, 482: 121–130. <https://doi.org/10.1016/j.chemgeo.2018.02.011>
- Huang, J.P., Liu, X.Y., He, Y.S., et al., 2021. The Oxygen Cycle and a Habitable Earth. *Science China: Earth Sciences*, 54(4):478–506 (in Chinese).
- Jeandel, C., Minster, J.F., 1987. Chromium Behavior in the Ocean: Global versus Regional Processes. *Global Biogeochemical Cycles*, 1(2): 131–154. <https://doi.org/10.1029/gb001i002p00131>
- Johnson, C.M., Beard, B.L., 2006. Fe Isotopes: An Emerging Technique for Understanding Modern and Ancient Biogeochemical Cycles. *GSA Today*, 16(11): 4. <https://doi.org/10.1130/gsat01611a.1>
- Jost, A.B., Bachan, A., van de Schootbrugge, B., et al., 2017. Uranium Isotope Evidence for an Expansion of Marine Anoxia during the End-Triassic Extinction. *Geochemistry, Geophysics, Geosystems*, 18(8): 3093–3108. <https://doi.org/10.1002/2017gc006941>
- Kadoya, S., Catling, D.C., Nicklas, R.W., et al., 2020. Mantle Data Imply a Decline of Oxidizable Volcanic Gases could have Triggered the Great Oxidation. *Nature Communications*, 11: 2774. <https://doi.org/10.1038/s41467-020-16493-1>
- Kendall, B., 2021. Recent Advances in Geochemical Paleooxybarometers. *Annual Review of Earth and Planetary Sciences*, 49:399–433. <https://doi.org/10.1146/annurev-earth-071520-051637>
- Kendall, B., Brennecka, G.A., Weyer, S., et al., 2013. Uranium Isotope Fractionation Suggests Oxidative Uranium Mobilization at 2.50 Ga. *Chemical Geology*, 362: 105–114. <https://doi.org/10.1016/j.chemgeo.2013.08.010>
- Kendall, B., Creaser, R.A., Gordon, G.W., et al., 2009. Re-Os and Mo Isotope Systematics of Black Shales from the Middle Proterozoic Velkerri and Wollgorang Formations, McArthur Basin, Northern Australia. *Geochimica et Cosmochimica Acta*, 73(9): 2534–2558. <https://doi.org/10.1016/j.gca.2009.02.013>
- Kendall, B., Dahl, T.W., Anbar, A.D., 2017. The Stable Isotope Geochemistry of Molybdenum. *Reviews in Mineralogy and Geochemistry*, 82(1):683–732. <https://doi.org/10.2138/rmg.2017.82.16>

- Kendall, B., Gordon, G. W., Poulton, S. W., et al., 2011. Molybdenum Isotope Constraints on the Extent of Late Paleoproterozoic Ocean Euxinia. *Earth and Planetary Science Letters*, 307(3–4): 450–460. <https://doi.org/10.1016/j.epsl.2011.05.019>
- Kendall, B., Komiya, T., Lyons, T. W., et al., 2015. Uranium and Molybdenum Isotope Evidence for an Episode of Widespread Ocean Oxygenation during the Late Ediacaran Period. *Geochimica et Cosmochimica Acta*, 156: 173–193. <https://doi.org/10.1016/j.gca.2015.02.025>
- Kendall, B., Wang, J. Y., Zheng, W., et al., 2020. Inverse Correlation between the Molybdenum and Uranium Isotope Compositions of Upper Devonian Black Shales Caused by Changes in Local Depositional Conditions rather than Global Ocean Redox Variations. *Geochimica et Cosmochimica Acta*, 287: 141–164. <https://doi.org/10.1016/j.gca.2020.01.026>
- Kirschvink, J. L., Kopp, R. E., 2008. Palaeoproterozoic Ice Houses and the Evolution of Oxygen-Mediating Enzymes: The Case for a Late Origin of Photosystem II. *Philosophical Transactions of the Royal Society B: Biological Sciences*, 363(1504): 2755–2765. <https://doi.org/10.1098/rstb.2008.0024>
- Knoll, A. H., Bergmann, K. D., Strauss, J. V., 2016. Life: The First Two Billion Years. *Philosophical Transactions of the Royal Society B: Biological Sciences*, 371(1707). <https://doi.org/10.1098/rstb.2015.0493>
- Kotaš, J., Stasicka, Z., 2000. Chromium Occurrence in the Environment and Methods of Its Speciation. *Environmental Pollution*, 107(3): 263–283. [https://doi.org/10.1016/S0269-7491\(99\)00168-2](https://doi.org/10.1016/S0269-7491(99)00168-2)
- Kurzweil, F., Drost, K., Pašava, J., et al., 2015a. Coupled Sulfur, Iron and Molybdenum Isotope Data from Black Shales of the Teplá-Barrandian Unit Argue against Deep Ocean Oxygenation during the Ediacaran. *Geochimica et Cosmochimica Acta*, 171: 121–142. <https://doi.org/10.1016/j.gca.2015.08.022>
- Kurzweil, F., Wille, M., Schoenberg, R., et al., 2015b. Continuously Increasing  $\delta^{98}\text{Mo}$  Values in Neoproterozoic Black Shales and Iron Formations from the Hamersley Basin. *Geochimica et Cosmochimica Acta*, 164: 523–542. <https://doi.org/10.1016/j.gca.2015.05.009>
- Kurzweil, F., Wille, M., Gantert, N., et al., 2016. Manganese Oxide Shuttling in Pre-GOE Oceans: Evidence from Molybdenum and Iron Isotopes. *Earth and Planetary Science Letters*, 452: 69–78. <https://doi.org/10.1016/j.epsl.2016.07.013>
- Lalonde, S. V., Konhauser, K. O., 2015. Benthic Perspective on Earth's Oldest Evidence for Oxygenic Photosynthesis. *Proceeding of the National Academy of Sciences*, 112(4): 995–1000. <https://doi.org/10.1073/pnas.1415718112>
- Large, R., 2014. The Boring Billion. *Australasian Science*, 35(4): 22–25. <https://doi.org/10.3316/iela-pa.520236687944675>
- Lau, K. V., MacDonald, F. A., Maher, K., et al., 2017. Uranium Isotope Evidence for Temporary Ocean Oxygenation in the Aftermath of the Sturtian Snowball Earth. *Earth and Planetary Science Letters*, 458: 282–292. <https://doi.org/10.1016/j.epsl.2016.10.043>
- Lau, K. V., Romaniello, S. J., Zhang, F. F., 2019. The Uranium Isotope Paleoredox Proxy. In: Lyons, T. W., Turchyn, A. V., Reinhard, C. T., eds., *Elements in Geochemical Tracers in Earth System Science*. Cambridge University Press, Cambridge.
- Lau, K. V., Lyons, T. W., Maher, K., 2020. Uranium Reduction and Isotopic Fractionation in Reducing Sediments: Insights from Reactive Transport Modeling. *Geochimica et Cosmochimica Acta*, 287: 65–92. <https://doi.org/10.1016/j.gca.2020.01.021>
- Lee, C. T. A., Yeung, L. Y., McKenzie, N. R., et al., 2016. Two-Step Rise of Atmospheric Oxygen Linked to the Growth of Continents. *Nature Geoscience*, 9(6): 417–424. <https://doi.org/10.1038/ngeo2707>
- Lehmann, B., Nägler, T. F., Holland, H. D., et al., 2007. Highly Metalliferous Carbonaceous Shale and Early Cambrian Seawater. *Geology*, 35(5): 403–406. <https://doi.org/10.1130/G23543a.1>
- Li, C., Cheng, M., Zhu, M. Y., et al., 2018. Heterogeneous and Dynamic Marine Shelf Oxygenation and Coupled Early Animal Evolution. *Emerging Topics in Life Sciences*, 2(2): 279–288. <https://doi.org/10.1042/etls20170157>
- Li, C., Love, G. D., Lyons, T. W., et al., 2010. A Stratified Redox Model for the Ediacaran Ocean. *Science*, 328(5974): 80–83. <https://doi.org/10.1126/science.1182369>
- Li, Z. H., Cao, M. C., Loyd, S. J., et al., 2020. Transient and Stepwise Ocean Oxygenation during the Late Ediacaran Shuram Excursion: Insights from Carbonate  $\delta^{238}\text{U}$  of Northwestern Mexico. *Precambrian Research*, 344: 105741. <https://doi.org/10.1016/j.precamres.2020.105741>
- Love, G. D., Grosjean, E., Stalvies, C., et al., 2009. Fossil Steroids Record the Appearance of Demospongiae during the Cryogenian Period. *Nature*, 457: 718–721. <https://doi.org/10.1038/nature07673>

- Lu, X.Z., Kendall, B., Stein, H.J., et al., 2017. Marine Redox Conditions during Deposition of Late Ordovician and Early Silurian Organic-Rich Mudrocks in the Siljan Ring District, Central Sweden. *Chemical Geology*, 457: 75–94. <https://doi.org/10.1016/j.chemgeo.2017.03.015>
- Luo, J., Long, X.P., Bowyer, F.T., et al., 2021. Pulsed Oxygenation Events Drove Progressive Oxygenation of the Early Mesoproterozoic Ocean. *Earth and Planetary Science Letters*, 559: 116754. <https://doi.org/10.1016/j.epsl.2021.116754>
- Lyons, T.W., Reinhard, C.T., Planavsky, N.J., 2014. The Rise of Oxygen in Earth's Early Ocean and Atmosphere. *Nature*, 506: 307–315. <https://doi.org/10.1038/nature13068>
- Mänd, K., Lalonde, S.V., Robbins, L.J., et al., 2020. Palaeoproterozoic Oxygenated Oceans Following the Lomagundi-Jatuli Event. *Nature Geoscience*, 13(4):302–306. <https://doi.org/10.1038/s41561-020-0558-5>
- Miller, C.A., Peucker-Ehrenbrink, B., Walker, B.D., et al., 2011. Re-Assessing the Surface Cycling of Molybdenum and Rhenium. *Geochimica et Cosmochimica Acta*, 75(22): 7146–7179. <https://doi.org/10.1016/j.gca.2011.09.005>
- Montoya-Pino, C., Weyer, S., Anbar, A.D., et al., 2010. Global Enhancement of Ocean Anoxia during Oceanic Anoxic Event 2: A Quantitative Approach Using U Isotopes. *Geology*, 38(4): 315–318. <https://doi.org/10.1130/g30652.1>
- Mukherjee, I., Large, R.R., Corkrey, R., et al., 2018. The Boring Billion, a Slingshot for Complex Life on Earth. *Scientific Reports*, 8(1):1–7. <https://doi.org/10.1038/s41598-018-22695-x>
- Nägler, T.F., Neubert, N., Böttcher, M.E., et al., 2011. Molybdenum Isotope Fractionation in Pelagic Euxinia: Evidence from the Modern Black and Baltic Seas. *Chemical Geology*, 289(1–2): 1–11. <https://doi.org/10.1016/j.chemgeo.2011.07.001>
- Nakagawa, Y., Takano, S., Firdaus, M.L., et al., 2012. The Molybdenum Isotopic Composition of the Modern Ocean. *Geochemical Journal*, 46(2): 131–141. <https://doi.org/10.2343/geochemj.1.0158>
- Neely, R.A., Gislason, S.R., Ólafsson, M., et al., 2018. Molybdenum Isotope Behaviour in Groundwaters and Terrestrial Hydrothermal Systems, Iceland. *Earth and Planetary Science Letters*, 486:108–118. <https://doi.org/10.1016/j.epsl.2017.11.053>
- Neubert, N., Heri, A.R., Voegelin, A.R., et al., 2011. The Molybdenum Isotopic Composition in River Water: Constraints from Small Catchments. *Earth and Planetary Science Letters*, 304(1–2): 180–190. <https://doi.org/10.1016/j.epsl.2011.02.001>
- Neubert, N., Nägler, T.F., Böttcher, M.E., 2008. Sulfidity Controls Molybdenum Isotope Fractionation into Euxinic Sediments: Evidence from the Modern Black Sea. *Geology*, 36(10): 775–778. <https://doi.org/10.1130/g24959a.1>
- Nielsen, S.G., Goff, M., Hesselbo, S.P., et al., 2011. Thallium Isotopes in Early Diagenetic Pyrite: A Paleoredox Proxy? *Geochimica et Cosmochimica Acta*, 75(21): 6690–6704. <https://doi.org/10.1016/j.gca.2011.07.047>
- Nielsen, S.G., Rehkämper, M., Norman, M.D., et al., 2006a. Thallium Isotopic Evidence for Ferromanganese Sediments in the Mantle Source of Hawaiian Basalts. *Nature*, 439:314–317. <https://doi.org/10.1038/nature04450>
- Nielsen, S.G., Rehkämper, M., Teagle, D.A.H., et al., 2006b. Hydrothermal Fluid Fluxes Calculated from the Isotopic Mass Balance of Thallium in the Ocean Crust. *Earth and Planetary Science Letters*, 251(1–2): 120–133. <https://doi.org/10.1016/j.epsl.2006.09.002>
- Nielsen, S.G., Rehkämper, M., Porcelli, D., et al., 2005. Thallium Isotope Composition of the Upper Continental Crust and Rivers: An Investigation of the Continental Sources of Dissolved Marine Thallium. *Geochimica et Cosmochimica Acta*, 69(8):2007–2019. <https://doi.org/10.1016/j.gca.2004.10.025>
- Nielsen, S.G., Rehkämper, M., Prytulak, J., 2017. Investigation and Application of Thallium Isotope Fractionation. *Reviews in Mineralogy and Geochemistry*, 82(1): 759–798. <https://doi.org/10.2138/rmg.2017.82.18>
- Nielsen, S.G., Wasylenko, L.E., Rehkämper, M., et al., 2013. Towards an Understanding of Thallium Isotope Fractionation during Adsorption to Manganese Oxides. *Geochimica et Cosmochimica Acta*, 117: 252–265. <https://doi.org/10.1016/j.gca.2013.05.004>
- Noordmann, J., Weyer, S., Montoya-Pino, C., et al., 2015. Uranium and Molybdenum Isotope Systematics in Modern Euxinic Basins: Case Studies from the Central Baltic Sea and the Kyllaren Fjord (Norway). *Chemical Geology*, 396: 182–195. <https://doi.org/10.1016/j.chemgeo.2014.12.012>
- Ossa Ossa, F., Eickmann, B., Hofmann, A., et al., 2018a. Two-Step Deoxygenation at the End of the Paleoproterozoic Lomagundi Event. *Earth and Planetary Science Letters*, 486: 70–83. <https://doi.org/10.1016/j.epsl.2018.01.009>

- Ossa Ossa, F., Hofmann, A., Wille, M., et al., 2018b. Aerobic Iron and Manganese Cycling in a Redox-Stratified Mesoproterozoic Epicontinental Sea. *Earth and Planetary Science Letters*, 500: 28–40. <https://doi.org/10.1016/j.epsl.2018.07.044>
- Ostrander, C. M., Johnson, A. C., Anbar, A. D., 2021. Earth's First Redox Revolution. *Annual Review of Earth and Planetary Sciences*, 49: 337–366. <https://doi.org/10.1146/annurev-earth-072020-055249>
- Ostrander, C. M., Nielsen, S. G., Owens, J. D., et al., 2019a. Fully Oxygenated Water Columns over Continental Shelves before the Great Oxidation Event. *Nature Geoscience*, 12(3): 186–191. <https://doi.org/10.1038/s41561-019-0309-7>
- Ostrander, C. M., Sahoo, S. K., Kendall, B., et al., 2019b. Multiple Negative Molybdenum Isotope Excursions in the Doushantuo Formation (South China) Fingerprint Complex Redox-Related Processes in the Ediacaran Nanhua Basin. *Geochimica et Cosmochimica Acta*, 261:191–209. <https://doi.org/10.1016/j.gca.2019.07.016>
- Ostrander, C. M., Owens, J. D., Nielsen, S. G., 2017. Constraining the Rate of Oceanic Deoxygenation Leading up to a Cretaceous Oceanic Anoxic Event (OAE-2: ~94 Ma). *Science Advances*, 3(8): e1701020. <https://doi.org/10.1126/sciadv.1701020>
- Ostrander, C. M., Owens, J. D., Nielsen, S. G., et al., 2020. Thallium Isotope Ratios in Shales from South China and Northwestern Canada Suggest Widespread O<sub>2</sub> Accumulation in Marine Bottom Waters was an Uncommon Occurrence during the Ediacaran Period. *Chemical Geology*, 557: 119856. <https://doi.org/10.1016/j.chemgeo.2020.119856>
- Owens, J. D., 2019. Application of Thallium Isotopes: Tracking Marine Oxygenation through Manganese Oxide Burial. In: Lyons, T. W., Turchyn, A. V., Reinhard, C. T., eds., *Elements in Geochemical Tracers in Earth System Science*. Cambridge University Press, Cambridge.
- Owens, J. D., Nielsen, S. G., Horner, T. J., et al., 2017. Thallium-Isotopic Compositions of Euxinic Sediments as a Proxy for Global Manganese-Oxide Burial. *Geochimica et Cosmochimica Acta*, 213: 291–307. <https://doi.org/10.1016/j.gca.2017.06.041>
- Partin, C. A., Bekker, A., Planavsky, N. J., et al., 2013. Large-Scale Fluctuations in Precambrian Atmospheric and Oceanic Oxygen Levels from the Record of U in Shales. *Earth and Planetary Science Letters*, 369–370: 284–293. <https://doi.org/10.1016/j.epsl.2013.03.031>
- Paulukat, C., Gilleaudeau, G. J., Chernyavskiy, P., et al., 2016. The Cr-Isotope Signature of Surface Seawater: A Global Perspective. *Chemical Geology*, 444: 101–109. <https://doi.org/10.1016/j.chemgeo.2016.10.004>
- Peacock, C. L., Moon, E. M., 2012. Oxidative Scavenging of Thallium by Birnessite: Explanation for Thallium Enrichment and Stable Isotope Fractionation in Marine Ferromanganese Precipitates. *Geochimica et Cosmochimica Acta*, 84: 297–313. <https://doi.org/10.1016/j.gca.2012.01.036>
- Pearce, C. R., Burton, K. W., von Strandmann, P. A. E. P., et al., 2010. Molybdenum Isotope Behaviour Accompanying Weathering and Riverine Transport in a Basaltic Terrain. *Earth and Planetary Science Letters*, 295(1–2): 104–114. <https://doi.org/10.1016/j.epsl.2010.03.032>
- Phan, T. T., Gardiner, J. B., Capo, R. C., et al., 2018. Geochemical and Multi-Isotopic (<sup>87</sup>Sr/<sup>86</sup>Sr, <sup>143</sup>Nd/<sup>144</sup>Nd, <sup>238</sup>U/<sup>235</sup>U) Perspectives of Sediment Sources, Depositional Conditions, and Diagenesis of the Marcellus Shale, Appalachian Basin, USA. *Geochimica et Cosmochimica Acta*, 222: 187–211. <https://doi.org/10.1016/j.gca.2017.10.021>
- Planavsky, N. J., Asael, D., Hofmann, A., et al., 2014a. Evidence for Oxygenic Photosynthesis Half a Billion Years before the Great Oxidation Event. *Nature Geoscience*, 7(4):283–286. <https://doi.org/10.1038/ngeo2122>
- Planavsky, N. J., Reinhard, C. T., Wang, X., et al., 2014b. Low Mid-Proterozoic Atmospheric Oxygen Levels and the Delayed Rise of Animals. *Science*, 346(6209): 635–638. <https://doi.org/10.1126/science.1258410>
- Planavsky, N. J., Slack, J. F., Cannon, W. F., et al., 2018. Evidence for Episodic Oxygenation in a Weakly Redox-Buffered Deep Mid-Proterozoic Ocean. *Chemical Geology*, 483: 581–594. <https://doi.org/10.1016/j.chemgeo.2018.03.028>
- Poulson Brucker, R. L., McManus, J., Poulton, S. W., 2012. Molybdenum Isotope Fractionations Observed under Anoxic Experimental Conditions. *Geochemical Journal*, 46(3):201–209. <https://doi.org/10.2343/geochemj.1.0167>
- Poulson Brucker, R. L., McManus, J., Severmann, S., et al., 2009. Molybdenum Behavior during Early Diagenesis: Insights from Mo Isotopes. *Geochemistry, Geophysics, Geosystems*, 10(6): Q06010. <https://doi.org/10.1029/2008gc002180>
- Poulton, S. W., 2017. Early Phosphorus Redigested. *Nature Geoscience*, 10(2): 75–76. <https://doi.org/10.1038/ngeo2884>

- Poulton, S. W., Bekker, A., Cumming, V. M., et al., 2021. A 200-Million-Year Delay in Permanent Atmospheric Oxygenation. *Nature*, 592: 232–236. <https://doi.org/10.1038/s41586-021-03393-7>
- Poulton, S. W., Fralick, P. W., Canfield, D. E., 2010. Spatial Variability in Oceanic Redox Structure 1.8 Billion Years Ago. *Nature Geoscience*, 3(7): 486–490. <https://doi.org/10.1038/ngeo889>
- Qin, L. P., Wang, X. L., 2017. Chromium Isotope Geochemistry. *Reviews in Mineralogy and Geochemistry*, 82(1): 379–414. <https://doi.org/10.2138/rmg.2017.82.10>
- Reinhard, C. T., Lalonde, S. V., Lyons, T. W., 2013. Oxidative Sulfide Dissolution on the Early Earth. *Chemical Geology*, 362: 44–55. <https://doi.org/10.1016/j.chemgeo.2013.10.006>
- Reinhard, C. T., Planavsky, N. J., Wang, X. L., et al., 2014. The Isotopic Composition of Authigenic Chromium in Anoxic Marine Sediments: A Case Study from the Cariaco Basin. *Earth and Planetary Science Letters*, 407: 9–18. <https://doi.org/10.1016/j.epsl.2014.09.024>
- Reinhard, C. T., Raiswell, R., Scott, C., et al., 2009. A Late Archean Sulfidic Sea Stimulated by Early Oxidative Weathering of the Continents. *Science*, 326(5953): 713–716. <https://doi.org/10.1126/science.1176711>
- Rimstidt, J. D., Vaughan, D. J., 2003. Pyrite Oxidation: A State-of-the-Art Assessment of the Reaction Mechanism. *Geochimica et Cosmochimica Acta*, 67(5): 873–880. [https://doi.org/10.1016/S0016-7037\(02\)01165-1](https://doi.org/10.1016/S0016-7037(02)01165-1)
- Robbins, L. J., Lalonde, S. V., Planavsky, N. J., et al., 2016. Trace Elements at the Intersection of Marine Biological and Geochemical Evolution. *Earth-Science Reviews*, 163: 323–348. <https://doi.org/10.1016/j.earsci-rev.2016.10.013>
- Rodler, A. S., Frei, R., Gaucher, C., et al., 2016. Chromium Isotope, REE and Redox-Sensitive Trace Element Chemostratigraphy across the Late Neoproterozoic Ghaub Glaciation, Otavi Group, Namibia. *Precambrian Research*, 286: 234–249. <https://doi.org/10.1016/j.precamres.2016.10.007>
- Rolison, J. M., Stirling, C. H., Middag, R., et al., 2017. Uranium Stable Isotope Fractionation in the Black Sea: Modern Calibration of the  $^{238}\text{U}/^{235}\text{U}$  Paleo-Redox Proxy. *Geochimica et Cosmochimica Acta*, 203: 69–88. <https://doi.org/10.1016/j.gca.2016.12.014>
- Romaniello, S. J., Herrmann, A. D., Anbar, A. D., 2013. Uranium Concentrations and  $^{238}\text{U}/^{235}\text{U}$  Isotope Ratios in Modern Carbonates from the Bahamas: Assessing a Novel Paleoredox Proxy. *Chemical Geology*, 362: 305–316. <https://doi.org/10.1016/j.chemgeo.2013.10.002>
- Romaniello, S. J., Herrmann, A. D., Anbar, A. D., 2016. Syndepositional Diagenetic Control of Molybdenum Isotope Variations in Carbonate Sediments from the Bahamas. *Chemical Geology*, 438: 84–90. <https://doi.org/10.1016/j.chemgeo.2016.05.019>
- Rooney, A. D., Cantine, M. D., Bergmann, K. D., et al., 2020. Calibrating the Coevolution of Ediacaran Life and Environment. *Proceedings of the National Academy of Sciences of the United States of America*, 117(29): 16824–16830. <https://doi.org/10.1073/pnas.2002918117>
- Rosing, M. T., Frei, R., 2004. U-Rich Archean Sea-Floor Sediments from Greenland - Indications of >3 700 Ma Oxygenic Photosynthesis. *Earth and Planetary Science Letters*, 217(3–4): 237–244. [https://doi.org/10.1016/S0012-821X\(03\)00609-5](https://doi.org/10.1016/S0012-821X(03)00609-5)
- Sahoo, S. K., Planavsky, N. J., Jiang, G., et al., 2016. Oceanic Oxygenation Events in the Anoxic Ediacaran Ocean. *Geobiology*, 14(5): 457–468. <https://doi.org/10.1111/gbi.12182>
- Sahoo, S. K., Planavsky, N. J., Kendall, B., et al., 2012. Ocean Oxygenation in the Wake of the Marinoan Glaciation. *Nature*, 489: 546–549. <https://doi.org/10.1038/nature11445>
- Sarmiento, J. L., Gruber, N., 2006. Ocean Biogeochemical Dynamics. Princeton University Press, Princeton.
- Schauble, E. A., 2007. Role of Nuclear Volume in Driving Equilibrium Stable Isotope Fractionation of Mercury, Thallium, and Other Very Heavy Elements. *Geochimica et Cosmochimica Acta*, 71(9): 2170–2189. <https://doi.org/10.1016/j.gca.2007.02.004>
- Scheiderich, K., Zerkle, A. L., Helz, G. R., et al., 2010. Molybdenum Isotope, Multiple Sulfur Isotope, and Redox-Sensitive Element Behavior in Early Pleistocene Mediterranean Sapropels. *Chemical Geology*, 279(3–4): 134–144. <https://doi.org/10.1016/j.chemgeo.2010.10.015>
- Schoenberg, R., Zink, S., Staubwasser, M., et al., 2008. The Stable Cr Isotope Inventory of Solid Earth Reservoirs Determined by Double Spike MC-ICP-MS. *Chemical Geology*, 249(3–4): 294–306. <https://doi.org/10.1016/j.chemgeo.2008.01.009>
- Scholz, F., Baum, M., Siebert, C., et al., 2018. Sedimentary Molybdenum Cycling in the Aftermath of Seawater Inflow to the Intermittently Euxinic Gotland Deep, Central Baltic Sea. *Chemical Geology*, 491: 27–38. <https://doi.org/10.1016/j.chemgeo.2018.04.031>

- Scott, C., Lyons, T. W., Bekker, A., et al., 2008. Tracing the Stepwise Oxygenation of the Proterozoic Ocean. *Nature*, 452(7186): 456–459. <https://doi.org/10.1038/nature06811>
- Shi, W., Li, C., Luo, G. M., et al., 2018. Sulfur Isotope Evidence for Transient Marine Shelf Oxidation during the Ediacaran Shuram Excursion. *Geology*, 46(3): 267–270. <https://doi.org/10.1130/g39663.1>
- Shields-Zhou, G., Och, L., 2011. The Case for a Neoproterozoic Oxygenation Event: Geochemical Evidence and Biological Consequences. *GSA Today*, 21(3): 4–11. <https://doi.org/10.1130/gsatg102a.1>
- Siebert, C., Kramers, J. D., Meisel, T., et al., 2005. PGE, Re-Os, and Mo Isotope Systematics in Archean and Early Proterozoic Sedimentary Systems as Proxies for Redox Conditions of the Early Earth. *Geochimica et Cosmochimica Acta*, 69(7): 1787–1801. <https://doi.org/10.1016/j.gca.2004.10.006>
- Siebert, C., McManus, J., Bice, A., et al., 2006. Molybdenum Isotope Signatures in Continental Margin Marine Sediments. *Earth and Planetary Science Letters*, 241(3–4): 723–733. <https://doi.org/10.1016/j.epsl.2005.11.010>
- Siebert, C., Nägler, T. F., von Blanckenburg, F., et al., 2003. Molybdenum Isotope Records as a Potential New Proxy for Paleoceanography. *Earth and Planetary Science Letters*, 211(1/2): 159–171. [https://doi.org/10.1016/s0012-821x\(03\)00189-4](https://doi.org/10.1016/s0012-821x(03)00189-4)
- Song, H. Y., Song, H. J., Algeo, T. J., et al., 2017. Uranium and Carbon Isotopes Document Global Ocean Redox-Productivity Relationships Linked to Cooling during the Frasnian-Famennian Mass Extinction. *Geology*, 45(10): 887–890. <https://doi.org/10.1130/g39393.1>
- Sperling, E. A., Wolock, C. J., Morgan, A. S., et al., 2015. Statistical Analysis of Iron Geochemical Data Suggests Limited Late Proterozoic Oxygenation. *Nature*, 523: 451–454. <https://doi.org/10.1038/nature14589>
- Stockey, R. G., Cole, D. B., Planavsky, N. J., et al., 2020. Persistent Global Marine Euxinia in the Early Silurian. *Nature Communications*, 11(1): 1–10. <https://doi.org/10.1038/s41467-020-15400-y>
- Stüeken, E. E., Buick, R., Guy, B. M., et al., 2015. Isotopic Evidence for Biological Nitrogen Fixation by Molybdenum-Nitrogenase from 3.2 Gyr. *Nature*, 520: 666–669. <https://doi.org/10.1038/nature14180>
- Stüeken, E. E., Kipp, M. A., Koehler, M. C., et al., 2016. The Evolution of Earth's Biogeochemical Nitrogen Cycle. *Earth-Science Reviews*, 160: 220–239. <https://doi.org/10.1016/j.earscirev.2016.07.007>
- Stylo, M., Neubert, N., Wang, Y., et al., 2015. Uranium Isotopes Fingerprint Biotic Reduction. *Proceedings of the National Academy of Sciences of the United States of America*, 112(18): 5619–5624. <https://doi.org/10.1073/pnas.1421841112>
- Tan, Z. Z., Jia, W. L., Li, J., et al., 2021. Geochemistry and Molybdenum Isotopes of the Basal Datangpo Formation: Implications for Ocean-Redox Conditions and Organic Matter Accumulation during the Cryogenian Interglaciation. *Palaeogeography, Palaeoclimatology, Palaeoecology*, 563: 110169. <https://doi.org/10.1016/j.palaeo.2020.110169>
- Them, T. R., Gill, B. C., Caruthers, A. H., et al., 2018. Thallium Isotopes Reveal Protracted Anoxia during the Toarcian (Early Jurassic) Associated with Volcanism, Carbon Burial, and Mass Extinction. *Proceedings of the National Academy of Science*, 115(26): 6596–6601. <https://doi.org/10.1073/pnas.1803478115>
- Thoby, M., Konhauser, K. O., Fralick, P. W., et al., 2019. Global Importance of Oxidic Molybdenum Sinks Prior to 2.6 Ga Revealed by the Mo Isotope Composition of Precambrian Carbonates. *Geology*, 47(6): 559–562. <https://doi.org/10.1130/g45706.1>
- Tissot, F. L. H., Chen, C., Go, B. M., et al., 2018. Controls of Eustasy and Diagenesis on the  $^{238}\text{U}/^{235}\text{U}$  of Carbonates and Evolution of the Seawater ( $^{234}\text{U}/^{238}\text{U}$ ) during the Last 1.4 Myr. *Geochimica et Cosmochimica Acta*, 242: 233–265. <https://doi.org/10.1016/j.gca.2018.08.022>
- Tissot, F. L. H., Dauphas, N., 2015. Uranium Isotopic Compositions of the Crust and Ocean: Age Corrections, U Budget and Global Extent of Modern Anoxia. *Geochimica et Cosmochimica Acta*, 167: 113–143. <https://doi.org/10.1016/j.gca.2015.06.034>
- Toma, J., Holmden, C., Shakotko, P., et al., 2019. Cr Isotopic Insights into ca. 1.9 Ga Oxidative Weathering of the Continents Using the Beaverlodge Lake Paleosol, Northwest Territories, Canada. *Geobiology*, 17(5): 467–489. <https://doi.org/10.1111/gbi.12342>
- Tossell, J. A., 2005. Calculating the Partitioning of the Isotopes of Mo between Oxidic and Sulfidic Species in Aqueous Solution. *Geochimica et Cosmochimica Acta*, 69(12): 2981–2993. <https://doi.org/10.1016/j.gca.2005.01.016>
- Tostevin, R., Clarkson, M. O., Gangl, S., et al., 2019. Uranium Isotope Evidence for an Expansion of Anoxia in Terminal Ediacaran Oceans. *Earth and Planetary Science Letters*, 510: 1–10. <https://doi.org/10.1016/j.epsl.2019.03.010>

- ters, 506: 104–112. <https://doi.org/10.1016/j.epsl.2018.10.045>
- Voegelin, A.R., Nägler, T.F., Beukes, N.J., et al., 2010. Molybdenum Isotopes in Late Archean Carbonate Rocks: Implications for Early Earth Oxygenation. *Precambrian Research*, 182(1–2): 70–82. <https://doi.org/10.1016/j.precamres.2010.07.001>
- Voegelin, A.R., Nägler, T.F., Samankassou, E., et al., 2009. Molybdenum Isotopic Composition of Modern and Carboniferous Carbonates. *Chemical Geology*, 265(3–4): 488–498. <https://doi.org/10.1016/j.chemgeo.2009.05.015>
- Wang, X.L., Ossa Ossa, F., Hofmann, A., et al., 2020. Uranium Isotope Evidence for Mesoarchean Biological Oxygen Production in Shallow Marine and Continental Settings. *Earth and Planetary Science Letters*, 551: 116583. <https://doi.org/10.1016/j.epsl.2020.116583>
- Wang, X.L., Planavsky, N.J., Hofmann, A., et al., 2018. A Mesoarchean Shift in Uranium Isotope Systematics. *Geochimica et Cosmochimica Acta*, 238: 438–452. <https://doi.org/10.1016/j.gca.2018.07.024>
- Wang, X.L., Planavsky, N.J., Reinhard, C.T., et al., 2016. A Cenozoic Seawater Redox Record Derived from  $^{238}\text{U}/^{235}\text{U}$  in Ferromanganese Crusts. *American Journal of Science*, 316(1): 64–83. <https://doi.org/10.2475/01.2016.02>
- Wang, X.L., Wei, W., 2020. Stable Chromium Isotope Geochemistry. *Earth Science Frontiers*, 27(3): 78–103 (in Chinese with English abstract).
- Wang, X.Q., Jiang, G.Q., Shi, X.Y., et al., 2018. Nitrogen Isotope Constraints on the Early Ediacaran Ocean Redox Structure. *Geochimica et Cosmochimica Acta*, 240: 220–235. <https://doi.org/10.1016/j.gca.2018.08.034>
- Wasylenki, L.E., Rolfe, B.A., Weeks, C.L., et al., 2008. Experimental Investigation of the Effects of Temperature and Ionic Strength on Mo Isotope Fractionation during Adsorption to Manganese Oxides. *Geochimica et Cosmochimica Acta*, 72(24): 5997–6005. <https://doi.org/10.1016/j.gca.2008.08.027>
- Wei, G.Y., Planavsky, N.J., He, T.C., et al., 2021a. Global Marine Redox Evolution from the Late Neoproterozoic to the Early Paleozoic Constrained by the Integration of Mo and U Isotope Records. *Earth-Science Reviews*, 214: 103506. <https://doi.org/10.1016/j.earsci-rev.2021.103506>
- Wei, G.Y., Planavsky, N.J., Tarhan, L.G., et al., 2018a. Marine Redox Fluctuation as a Potential Trigger for the Cambrian Explosion. *Geology*, 46(7): 587–590. <https://doi.org/10.1130/g40150.1>
- Wei, G.Y., Planavsky, N.J., Tarhan, L.G., et al., 2020. Highly Dynamic Marine Redox State through the Cambrian Explosion Highlighted by Authigenic  $\delta^{238}\text{U}$  Records. *Earth and Planetary Science Letters*, 544: 116361. <https://doi.org/10.1016/j.epsl.2020.116361>
- Wei, W., Frei, R., Chen, T.Y., et al., 2018b. Marine Ferromanganese Oxide: A Potentially Important Sink of Light Chromium Isotopes? *Chemical Geology*, 495: 90–103. <https://doi.org/10.1016/j.chemgeo.2018.08.006>
- Wei, W., Frei, R., Kläebe, R., et al., 2021b. A Transient Swing to Higher Oxygen Levels in the Atmosphere and Oceans at  $\sim 1.4$  Ga. *Precambrian Research*, 354: 106058. <https://doi.org/10.1016/j.precamres.2020.106058>
- Wen, H.J., Carignan, J., Zhang, Y.X., et al., 2011. Molybdenum Isotopic Records across the Precambrian-Cambrian Boundary. *Geology*, 39(8): 775–778. <https://doi.org/10.1130/g32055.1>
- Wen, H.J., Fan, H.F., Zhang, Y.X., et al., 2015. Reconstruction of Early Cambrian Ocean Chemistry from Mo Isotopes. *Geochimica et Cosmochimica Acta*, 164: 1–16. <https://doi.org/10.1016/j.gca.2015.05.008>
- White, D.A., Elrick, M., Romaniello, S., et al., 2018. Global Seawater Redox Trends during the Late Devonian Mass Extinction Detected Using U Isotopes of Marine Limestones. *Earth and Planetary Science Letters*, 503: 68–77. <https://doi.org/10.1016/j.epsl.2018.09.020>
- Willbold, M., Elliott, T., 2017. Molybdenum Isotope Variations in Magmatic Rocks. *Chemical Geology*, 449: 253–268. <https://doi.org/10.1016/j.chemgeo.2016.12.011>
- Wille, M., Kramers, J.D., Nägler, T.F., et al., 2007. Evidence for a Gradual Rise of Oxygen between 2.6 and 2.5 Ga from Mo Isotopes and Re-PGE Signatures in Shales. *Geochimica et Cosmochimica Acta*, 71(10): 2417–2435. <https://doi.org/10.1016/j.gca.2007.02.019>
- Wille, M., Nägler, T.F., Lehmann, B., et al., 2008. Hydrogen Sulphide Release to Surface Waters at the Precambrian/Cambrian Boundary. *Nature*, 453: 767–769. <https://doi.org/10.1038/nature07072>
- Wille, M., Nebel, O., van Kranendonk, M.J., et al., 2013. Mo-Cr Isotope Evidence for a Reducing Archean Atmosphere in 3.46–2.76 Ga Black Shales from the Pilbara, Western Australia. *Chemical Geology*, 340: 68–76. <https://doi.org/10.1016/j.chemgeo.2012.12.018>
- Xu, L.G., Lehmann, B., Mao, J.W., et al., 2012. Mo Isotope and Trace Element Patterns of Lower Cambrian Black

- Shales in South China: Multi-Proxy Constraints on the Paleoenvironment. *Chemical Geology*, 318/319: 45–59. <https://doi.org/10.1016/j.chemgeo.2012.05.016>
- Yang, S., Kendall, B., Lu, X.Z., et al., 2017. Uranium Isotope Compositions of Mid-Proterozoic Black Shales: Evidence for an Episode of Increased Ocean Oxygenation at 1.36 Ga and Evaluation of the Effect of Post-Depositional Hydrothermal Fluid Flow. *Precambrian Research*, 298: 187–201. <https://doi.org/10.1016/j.precamres.2017.06.016>
- Ye, Y.T., Wang, H.J., Wang, X.M., et al., 2020. Tracking the Evolution of Seawater Mo Isotopes through the Ediacaran-Cambrian Transition. *Precambrian Research*, 350: 105929. <https://doi.org/10.1016/j.precamres.2020.105929>
- Yin, H.F., Yu, J.X., Luo, G.M., et al., 2018. Biotic Influence on the Formation of Icehouse Climates in Geologic History. *Earth Science*, 43(11): 3809–3822 (in Chinese with English abstract).
- Yin, L., Li, J., Tian, H., et al., 2018. Rhenium-Osmium and Molybdenum Isotope Systematics of Black Shales from the Lower Cambrian Niutitang Formation, SW China: Evidence of a Well Oxygenated Ocean at ca. 520 Ma. *Chemical Geology*, 499: 26–42. <https://doi.org/10.1016/j.chemgeo.2018.08.016>
- Yusof, A.M., Chia, C.H., Wood, A.K.H., 2007. Speciation of Cr(III) and Cr(VI) in Surface Waters with a Chelex-100 Resin Column and Their Quantitative Determination Using Inductively Coupled Plasma Mass Spectrometry and Instrumental Neutron Activation Analysis. *Journal of Radioanalytical and Nuclear Chemistry*, 273(3): 533–538. <https://doi.org/10.1007/s10967-007-0904-8>
- Zhang, F.F., Algeo, T.J., Cui, Y., et al., 2019a. Global-Ocean Redox Variations across the Smithian-Spathian Boundary Linked to Concurrent Climatic and Biotic Changes. *Earth-Science Reviews*, 195: 147–168. <https://doi.org/10.1016/j.earscirev.2018.10.012>
- Zhang, F.F., Xiao, S.H., Romaniello, S.J., et al., 2019b. Global Marine Redox Changes Drove the Rise and Fall of the Ediacara Biota. *Geobiology*, 17(6): 594–610. <https://doi.org/10.1111/gbi.12359>
- Zhang, S.C., Wang, X.M., Wang, H.J., et al., 2019c. Paleoenvironmental Proxies and What the Xiamaling Formation Tells Us about the Mid-Proterozoic Ocean. *Geobiology*, 17(3): 225–246. <https://doi.org/10.1111/gbi.12337>
- Zhang, F.F., Algeo, T.J., Romaniello, S.J., et al., 2018a. Congruent Permian-Triassic  $\delta^{238}\text{U}$  Records at Panthalassic and Tethyan Sites: Confirmation of Global-Oceanic Anoxia and Validation of the U-Isotope Paleoredox Proxy. *Geology*, 46(4): 327–330. <https://doi.org/10.1130/g39695.1>
- Zhang, F.F., Romaniello, S.J., Algeo, T.J., et al., 2018b. Multiple Episodes of Extensive Marine Anoxia Linked to Global Warming and Continental Weathering Following the Latest Permian Mass Extinction. *Science Advances*, 4(4): e1602921. <https://doi.org/10.1126/sciadv.1602921>
- Zhang, F.F., Xiao, S.H., Kendall, B., et al., 2018c. Extensive Marine Anoxia during the Terminal Ediacaran Period. *Science Advances*, 4(6): eaan8983. <https://doi.org/10.1126/sciadv.aan8983>
- Zhang, F.F., Lenton, T.M., del Rey, Á., et al., 2020. Uranium Isotopes in Marine Carbonates as a Global Ocean Paleoredox Proxy: A Critical Review. *Geochimica et Cosmochimica Acta*, 287: 27–49. <https://doi.org/10.1016/j.gca.2020.05.011>
- Zhang, K., Zhu, X.K., Wood, R.A., et al., 2018. Oxygenation of the Mesoproterozoic Ocean and the Evolution of Complex Eukaryotes. *Nature Geoscience*, 11(5): 345–350. <https://doi.org/10.1038/s41561-018-0111-y>
- Zhang, S.C., Wang, X.M., Wang, H.J., et al., 2016. Sufficient Oxygen for Animal Respiration 1 400 Million Years Ago. *Proceedings of the National Academy of Sciences of the United States of America*, 113(7): 1731–1736. <https://doi.org/10.1073/pnas.1523449113>
- Zhao, X.K., Shi, X.Y., Wang, X.Q., et al., 2018. Stepwise Oxygenation of Early Cambrian Ocean Drove Early Metazoan Diversification. *Earth Science*, 43(11): 3873–3890 (in Chinese with English abstract).
- Zhou, L., Su, J., Huang, J.H., et al., 2011. A New Paleoenvironmental Index for Anoxic Events — Mo Isotopes in Black Shales from Upper Yangtze Marine Sediments. *Science China Earth Sciences*, 54(7): 1024–1033. <https://doi.org/10.1007/s11430-011-4188-z>
- Zhou, L., Wignall, P.B., Su, J., et al., 2012. U/Mo Ratios and  $\delta^{98/95}\text{Mo}$  as Local and Global Redox Proxies during Mass Extinction Events. *Chemical Geology*, 324–325: 99–107. <https://doi.org/10.1016/j.chemgeo.2012.03.020>
- Zhou, X.Q., Chen, D.Z., Liu, M., et al., 2017. The Future of Sedimentology in China: A Review and Perspective of Sedimentary Geochemistry. *Acta Sedimentologica Sinica*, 35(6): 1293–1316 (in Chinese with English abstract).
- Zhu, J.M., Zhu, X.K., Huang, F., 2008. The Systematics of Molybdenum Stable Isotope and Its Application to Earth



- Science. *Acta Petrologica et Mineralogica*, 27(4): 353—360(in Chinese with English abstract).
- Zhu, M. Y., 2010. The Origin and Cambrian Explosion of Animals: Fossil Evidences from China. *Acta Palaeontologica Sinica*, 49(3): 269—287(in Chinese with English abstract).
- Zhu, M. Y., Zhao, F. C., Yin, Z. J., et al., 2019. The Cambrian Explosion: Advances and Perspectives from China. *Science China Earth Sciences*, 49(10): 1455—1490(in Chinese with English abstract).
- Zhu, X. K., Wang, Y., Yan, B., et al., 2013. Developments of Non-Traditional Stable Isotope Geochemistry. *Bulletin of Mineralogy, Petrology and Geochemistry*, 32(6): 651—688(in Chinese with English abstract).
- Zink, S., Schoenberg, R., Staubwasser, M., 2010. Isotopic Fractionation and Reaction Kinetics between Cr(III) and Cr(VI) in Aqueous Media. *Geochimica et Cosmochimica Acta*, 74(20): 5729—5745. <https://doi.org/10.1016/j.gca.2010.07.015>
- 程猛, 李超, 周炼, 等, 2015. 钼海洋地球化学与古海洋化学重建. *中国科学:地球科学*, 45(11): 1649—1660.
- 黄建平, 刘晓岳, 何永胜, 等, 2021. 氧循环与宜居地球. *中国科学:地球科学*, 51(4): 487—506.
- 王相力, 卫炜, 2020. 铬稳定同位素地球化学. *地学前缘*, 27(3): 78—103.
- 殷鸿福, 喻建新, 罗根明, 等, 2018. 地史时期生物对冰室气候形成的作用. *地球科学*, 43(11): 3809—3822.
- 赵相宽, 史晓颖, 王新强, 等, 2018. 武纪早期海洋阶段性氧化驱动早期后生动物多样化进程. *地球科学*, 43(11): 3873—3890.
- 周锡强, 陈代钊, 刘牧, 等, 2017. 中国沉积学发展战略: 沉积地球化学研究现状与展望. *沉积学报*, 35(6): 1293—1316.
- 朱建明, 朱祥坤, 黄方, 2008. 钼的稳定同位素体系及其地质应用. *岩石矿物学杂志*, 27(4): 353—360.
- 朱茂炎, 2010. 动物的起源和寒武纪大爆发: 来自中国的化石证据. *古生物学报*, 49(3): 269—287.
- 朱茂炎, 赵方臣, 殷宗军, 等, 2019. 中国的寒武纪大爆发研究: 进展与展望. *中国科学:地球科学*, 49(10): 1455—1490.
- 朱祥坤, 王跃, 闫斌, 等, 2013. 非传统稳定同位素地球化学的创建与发展. *矿物岩石地球化学通报*, 32(6): 651—688.

#### 附中文参考文献

程猛, 李超, 周炼, 等, 2015. 钼海洋地球化学与古海洋化学重